Genetic variants associated with longitudinal changes in brain structure across the lifespan

Brouwer, R.M.; Klein, M.; Grasby, K.L.; Schnack, H.G.; Jahanshad, N.; Teeuw, J.; ... ; IMAGEN Consortium

nature neuroscience

ARTICLES

https://doi.org/10.1038/s41593-022-01042-4

Genetic variants associated with longitudinal changes in brain structure across the lifespan

Human brain structure changes throughout the lifespan. Altered brain growth or rates of decline are implicated in a vast range of psychiatric, developmental and neurodegenerative diseases. In this study, we identified common genetic variants that affect rates of brain growth or atrophy in what is, to our knowledge, the first genome-wide association meta-analysis of changes in brain morphology across the lifespan. Longitudinal magnetic resonance imaging data from 15,640 individuals were used to compute rates of change for 15 brain structures. The most robustly identified genes *GPR139*, *DACH1* and *APOE* are associated with metabolic processes. We demonstrate global genetic overlap with depression, schizophrenia, cognitive functioning, insomnia, height, body mass index and smoking. Gene set findings implicate both early brain development and neurodegenerative processes in the rates of brain changes. Identifying variants involved in structural brain changes may help to determine biological pathways underlying optimal and dysfunctional brain development and aging.

Under the influence of genes and a varying environment, human brain structure changes throughout the lifespan. Even in adulthood, when the brain seems relatively stable, individuals differ in the profile and rate of brain changes[1]. Longitudinal studies are crucial to identify genetic and environmental factors that influence the rate of these brain changes throughout development[2] and aging[3]. Inter-individual differences in brain development are associated with general cognitive function[4,5] and risk for psychiatric disorders[6,7] and neurological diseases[8,9]. Genetic factors involved in brain development and aging overlap with those for cognition[10] and risk for neuropsychiatric disorders[11]. A recent cross-sectional study showed brain age to be advanced in several brain disorders. Brain age is an estimate of biological age based on brain structure, which can deviate from chronological age. Several shared loci were found between the genome-wide association study (GWAS) summary statistics for advanced brain age and psychiatric disorders[12]. However, information is still lacking on which genetic variants influence an individual's brain changes throughout life, because this requires longitudinal data. Discovering genetic factors that explain variation between individuals in brain structural changes may reveal key biological pathways that drive normal development and aging and may contribute to identifying disease risk and resilience— a crucial goal given the urgent need for new treatments for aberrant brain development and aging worldwide.

As part of the Enhancing NeuroImaging Genetics through Meta-Analysis (ENIGMA) consortium[13], the ENIGMA Plasticity Working Group quantified the overall genetic contribution to longitudinal brain changes by combining evidence from multiple twin cohorts across the world[14]. Most global and subcortical brain measures showed genetic influences on change over time, with a higher genetic contribution in the elderly (heritability, 16–42%). Genetic factors that influence longitudinal changes were partially independent of those that influence baseline volumes of brain structures, suggesting that there might be genetic variants that specifically affect the rate of development or aging. However, the genes involved in these processes are still not known, with only a single, small-scale GWAS performed for longitudinal volume change in gray and white matter of the cerebrum, basal ganglia and cerebellum[15]. In this study, we set out to find genetic variants that may influence rates of brain changes over time, using genome-wide analysis in individuals scanned with magnetic resonance imaging (MRI) on more than one occasion. We also aimed to identify age-dependent effects of genomic variation on longitudinal brain changes in mostly healthy populations, but also populations with neurological and psychiatric disorders.

In our GWAS meta-analysis, we sought genetic loci associated with annual change rates in eight global and seven subcortical morphological brain measures in a coordinated two-phased analysis using data from 40 longitudinal cohorts (Extended Data Fig. 1 and Supplementary Table 1). We extracted global and subcortical brain measures, and assessed annual change rates, using additive genetic association analyses to estimate the effects of genetic variants on the rates of change within each cohort. As brain change is not constant over age[1], and gene expression also changes during development and aging[16], we determined whether the estimated genetic variants were age dependent—that is, differentially affected rates of brain changes at different stages of life—by using genome-wide meta-regression models with linear or quadratic age effects (Methods). It must be noted that, although the cohorts analyzed in this study together cover the full lifespan, there is relatively little age overlap between them. This implies that we cannot rule out that cohort-specific characteristics other than age could influence our meta-regression findings.

We employed a rolling cumulative meta-analysis and meta-regression approach[17]. In phase 1, for which data collection ended on 1 February 2019, we analyzed the cohorts of European descent ($n = 9{,}623$). We sought replication by adding data from three additional cohorts that became available after our analysis of phase 1: one developmental cohort (average age 10 years at baseline) and two in aging populations ($n = 5{,}477$; all of European descent) (total $n = 15{,}100$ in phase 2). For all follow-up analyses, we used results from phase 2. Finally, we added cohorts of non-European ancestry (total $n = 15{,}640$).

Longitudinal trajectories

Brain measures showed differing trajectories of change with age (Figs. 1 and 2 and Extended Data Video 1)—monotonic increases (lateral ventricles), monotonic decreases (cortex volume, cerebellar gray matter volume, cortical thickness, surface area and total brain volume) or increases followed by stabilization and subsequently decreases (cerebral and cerebellar white matter, thalamus, caudate, putamen, nucleus accumbens, pallidum, hippocampus and amygdala volumes). Each brain structure showed a characteristic trajectory of change. Within two of our largest cohorts in phase 1

A full list of author and affiliations appears at the end of the paper.

(one in childhood and one in older age), we computed correlations between the rates of change of all possible pairs of these 15 brain structures. These correlations in both childhood and older age were generally low in our data (Extended Data Fig. 2), except for the correlation between rates of change of cortical thickness and cortex volume. Therefore, we chose to investigate all brain structures separately, maximizing sensitivity of the GWAS to identify region-specific associations of genetic variants. Using the correlation structure, we estimated the effective number of independent variables through matrix spectral decomposition on the rates of change, yielding 14 independent traits for multiple testing corrections (Methods).

Age-independent associations

Two loci showed genome-wide significant effects on the rate of brain change in phase 1, one of which was also genome-wide significant in phase 2 (Fig. 3 and Supplementary Table 4; P value replication sample = 0.08). This lead single-nucleotide polymorphism (SNP), rs72772740 on chromosome 16, is an intronic variant located in the *GPR139* gene and was associated with rate of change in lateral ventricle volume (Fig. 4). Functional annotation identified many significant expression quantitative trait loci (eQTL) associations (false discovery rate (FDR) < 0.05) in different datasets and highlighted genes by either eQTL mapping (*GPRC5B*, *IQCK*, *KNOP1* and *C16orf62*) or chromatin interaction mapping (*ACSM1*, *ACSM5*, *UMOD* and *GP2*). *GPR139* is the G-protein-coupling receptor gene 139, which encodes a member of the rhodopsin family of G-protein-coupled receptors. The gene is almost exclusively expressed in the central nervous system, with highest expression from 12 to 26 weeks after conception, and has been suggested as a therapeutic target for metabolic syndromes and motor diseases[18]. *GPR139* may play a role in fetal brain development[19]. Mice lacking *GPR139* exhibited schizophrenia-like behavioral abnormalities[20], and functional cell assays showed the inhibitory influence of *GPR139* on dopamine receptor 2 signaling[20]. The second lead SNP, rs449998, an intronic variant on chromosome 21 located in the *DSCAM* (Down syndrome cell adhesion molecule) gene, was associated with the rate of change in nucleus accumbens volume in phase 1, but this association was not significant in the replication sample or phase 2. Three SNPs were significant in the phase 2 analysis only. These include rs10990953, intergenic on chromosome 9, associated with rate of change in lateral ventricle volume; rs1425034, intergenic and located in long intergenic non-protein-coding RNA on chromosome 2, associated with rate of change in pallidum volume; and rs12325429, intron of *CDH8* on chromosome 16, associated with rate of change in total brain volume (Supplementary Table 5; Supplementary Figs. 1 and 2 provide Manhattan plots, Q–Q plots, locus plots and circos plots). The association of *CDH8* with total brain volume rate of change is particularly interesting, because *CDH8* has been associated previously with learning disability and autism[21]. *CDH8* is a protein-coding gene and encodes a type II classical cadherin from the cadherin superfamily, integral membrane proteins that mediate calcium-dependent cell–cell adhesion. Genome-wide significant SNPs in phase 1 or phase 2 did not show heterogeneity ($I^2 < 10.2$; $p(I^2) > 0.31$; Supplementary Tables 4 and 5 and Supplementary Fig. 3 for forest plots).

Age-dependent associations

Three additional loci had an association with rate of change that was variable across the lifespan in phase 1 (Fig. 3 and Supplementary Tables 6 and 8). For two of these, the association remained significant in the phase 2 analysis: rate of change in white matter cerebrum volume was affected by rs573983368 (13:72353395, intronic variant) in the *DACH1* (Dachshund family transcription factor 1) gene, and 5:157751672 (intergenic and located in long intergenic non-protein-coding RNA LINC02227) on chromosome 5 had an age-dependent effect on the rate of change in surface area (Fig. 4 and Supplementary Tables 6–9). Rate of change in cerebellar white matter volume was affected by the intronic rs10674957 in the *TRHDE* (thyrotropin-releasing hormone-degrading enzyme) gene, but this third locus was not significant in phase 2.

The *DACH1* locus shows significant chromatin interaction, which can play an important role in gene expression regulation. *DACH1* encodes a chromatin-associated protein that associates with DNA-binding transcription factors to regulate gene expression and cell fate determination during development. *DACH1* is highly expressed in the proliferating neural progenitor cells of the developing cortical ventricular and subventricular regions and in the striatum[22]. We found the effect of *DACH1* to have a quadratic age dependence, with the variant being associated with faster growth in childhood and earlier but slower decline with aging (Fig. 4). The effect of 5:157751672 had a linear age dependence, with the tested variant being associated with less growth of surface area in childhood and less decline in older age.

For seven additional loci, we found a significant age-dependent association with rate of change only in phase 2 (Supplementary Tables 7 and 9; Supplementary Figs. 1 and 2 provide Manhattan plots, Q–Q plots, locus plots and circos plots). One of these, rs429358, a missense variant of the Alzheimer's disease (AD)-related[23] *APOE* (apolipoprotein E) gene, was associated with change rate in hippocampus, showing prolonged growth into adulthood and faster reductions of volume of the hippocampus for carriers of the AD risk variant. *APOE* plays a role in maintenance of cellular cholesterol homeostasis by delivering cholesterol to neurons on apoE-containing lipoprotein particles. Cholesterol is important for synapse and dendrite formation, and cholesterol depletion has been shown to cause synaptic and dendritic degeneration[24]. Other findings include rs12019523, an intronic variant in the *CAB39L* gene associated with rate of change of the caudate volume; rs34342646, an intronic variant in the *NECTIN2* gene associated with rate of change in surface area; and rs73210410, an intronic variant in the *SORCS2* gene associated with rate of change in pallidum volume.

To visualize the age-dependent effects, we plotted the meta-regression results for the significant loci (Methods and Supplementary Fig. 3). Genome-wide significant SNPs in phase 1 or phase 2 did not show significant residual heterogeneity ($P > 0.23$; except for the age-dependent effect of rs429358 on hippocampus change rate ($P = 0.02$)). A summary of the genome-wide significant results and the top ten loci for each phenotype and age model are presented in Supplementary Tables 4–9.

Gene-based analyses

Gene-based associations with all phenotypes were estimated using MAGMA (Methods). We found six genome-wide significant genes influencing structural rates of change in phase 1, four of which were also significant in phase 2 (Supplementary Tables 10 and 11); among these, *DACH1* and *GPR139*, which were implicated through SNP-based GWAS, also reached genome-wide significance in this gene-based GWAS. In addition, we found *APOE* to be associated with change rates for both hippocampus and amygdala. The phase 2 analysis showed two new findings: an association of the *FAU* gene with rate of change in cerebellum white matter volume and, again, *APOE*, associated with rate of change in surface area. Of note, the *APOE* findings were based on GWAS and subsequent gene analysis, and we did not investigate the classical *APOE* status, because that is determined by a combination of two SNPs. However, we observed that the effect of *APOE* on change rate of hippocampus and amygdala was fully driven by rs429358, with the risk variant for AD causing prolonged growth into adulthood and faster decay for both amygdala and hippocampus volumes later in life.

To visualize the age-dependent effects, we plotted the meta-regression results for the top SNP in each of the significant genes (Supplementary Fig. 3). Supplementary Tables 10 and 11 display the top ten genes for each phenotype and each age model. Supplementary

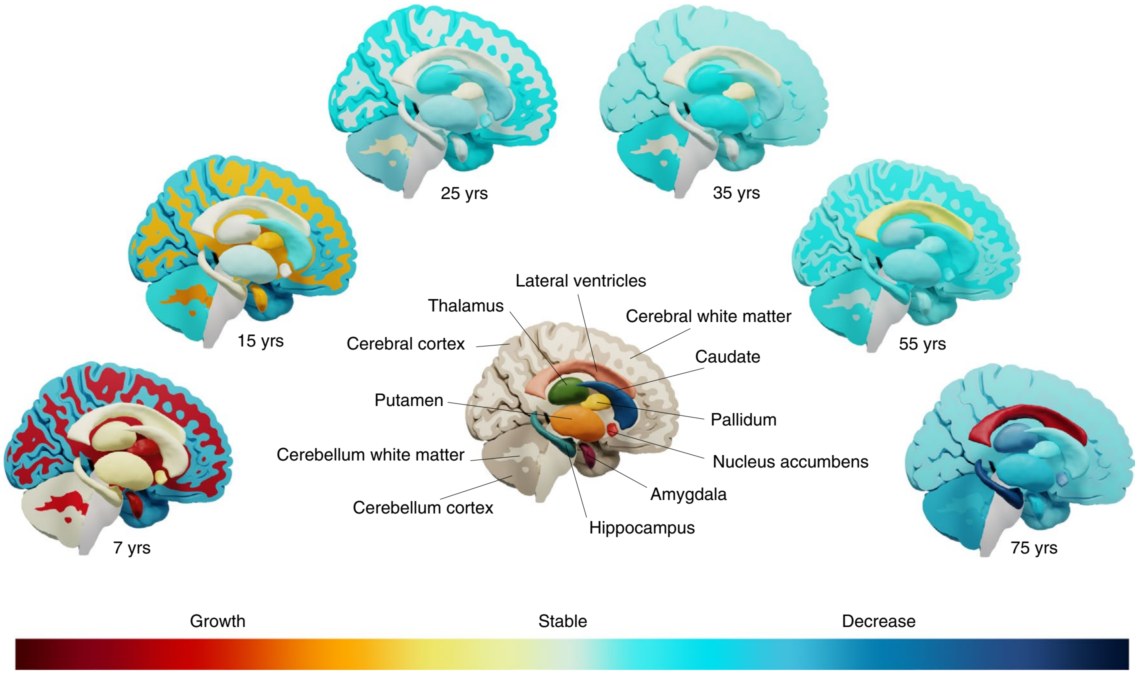

Fig. 1 | Phenotypic brain changes throughout the lifespan. Visualization of growth and decline of brain structures throughout the lifespan. The subcortical structures are shown in exploded view.

Table 12 details putative biological functions of associated genes and genes harboring genome-wide significant associated loci.

Gene set analyses

To test whether genetic findings for brain structure change converged onto functional gene sets and pathways, we conducted gene set analyses using MAGMA (Methods). Competitive testing was used, and ten and 12 genome-wide significant gene sets were found for phase 1 and phase 2, respectively (Supplementary Tables 13 and 14 for top ten gene sets and genes included). Two main themes emerge from this analysis, as biological functions of the gene sets converge onto involvement in early brain development and involvement in neurodegeneration, respectively.

One gene set was significant in both the phase 1 and phase 2 analyses—that is, GO_neural_nucleus_development. This gene set consists of genes involved in the development of neural nuclei (compact clusters of neurons in the brain) and was associated with rates of change in cerebellar white matter volume in our study. Two other gene sets, significant in phase 1 (GO_substantia_nigra_development associated with rate of change in cerebellum white matter volume) and phase 2 (GO_midbrain_development associated with quadratic age-dependent surface area rates of change) were closely related to neural nucleus development in Gene Ontology (GO) terms.

The most significant gene set was GO_response_to_phorbol_13_acetate_12_myristate ($P=1.42\times10^{-8}$) in phase 2, related to surface area change. Phorbol 13-acetate 12-myristate is a phorbol ester and an activator of protein kinase C (PKC)[25]. Two other gene sets, significant in phase 2 (GO_tau_protein_binding and GO_tau_protein_kinase_activity) and both associated with rate of change in caudate volume, imply genes involved in interacting with tau protein. Tau is a microtubule-associated protein, implicated in AD, Down syndrome and amyotrophic lateral sclerosis.

Follow-up analyses: overlap with cross-sectional findings

SNP-based heritability estimates (h^2) of the rates of change based on linkage disequilibrium score regression (LDSC; Methods) were small overall (Supplementary Table 15). For all phenotypes, the h^2 z-score was below 4. We, thus, tested for genetic overlap with cross-sectional brain data and other phenotypes by applying approaches other than LDSC, although these do not provide a measure of genetic correlation. To investigate whether cross-sectional GWAS for brain structure and our GWAS on rates of change identify the same or different genetic variants, we investigated overlap between rate of change and earlier published data on cross-sectional brain structure of the same structure, where available (Methods). Supplementary Fig. 4 displays the number of overlapping genes tested against the expected number of overlapping genes that would occur by chance, in the first 1–1,000 ranked genes. Supplementary Table 11 lists the top ten gene findings for each of the 15 change-rate phenotypes and compares these with the gene ranks from cross-sectional data. In the top ten ranked genes, *APOE* for hippocampus occurred in the top ten for both cross-sectional data[26] and age-dependent effects on rate of change ($P=0.006$). No overlap was seen for the other measured phenotypes. Extending this search to the top 200 (~1% of genes), we found overlapping genes above chance level for cortical thickness of quadratic age-dependent genes and cross-sectional findings ($P=8.39\times10^{-5}$). In the top 1,000 ranked genes (~5% of genes), further overlapping genes did emerge (Supplementary Fig. 4). Overlapping genes at such a high aggregate level imply that largely different genetic backgrounds underlie changes in brain structure and brain structure per se.

To test for global genomic overlap between our findings and GWAS of cross-sectional volumes, we applied independent SNP effect concordance analyses (iSECA) (Methods) and tested for pleiotropy. We found no significant pleiotropy between longitudinal and cross-sectional results, confirming a largely different genetic background for changes in brain structure and brain structure per se (Fig. 5).

Follow-up analyses: overlap with other traits

We applied iSECA for overlap between our age-independent summary statistics for structural brain changes and several neuropsychiatric, neurological, physical, aging and disease-related phenotypes

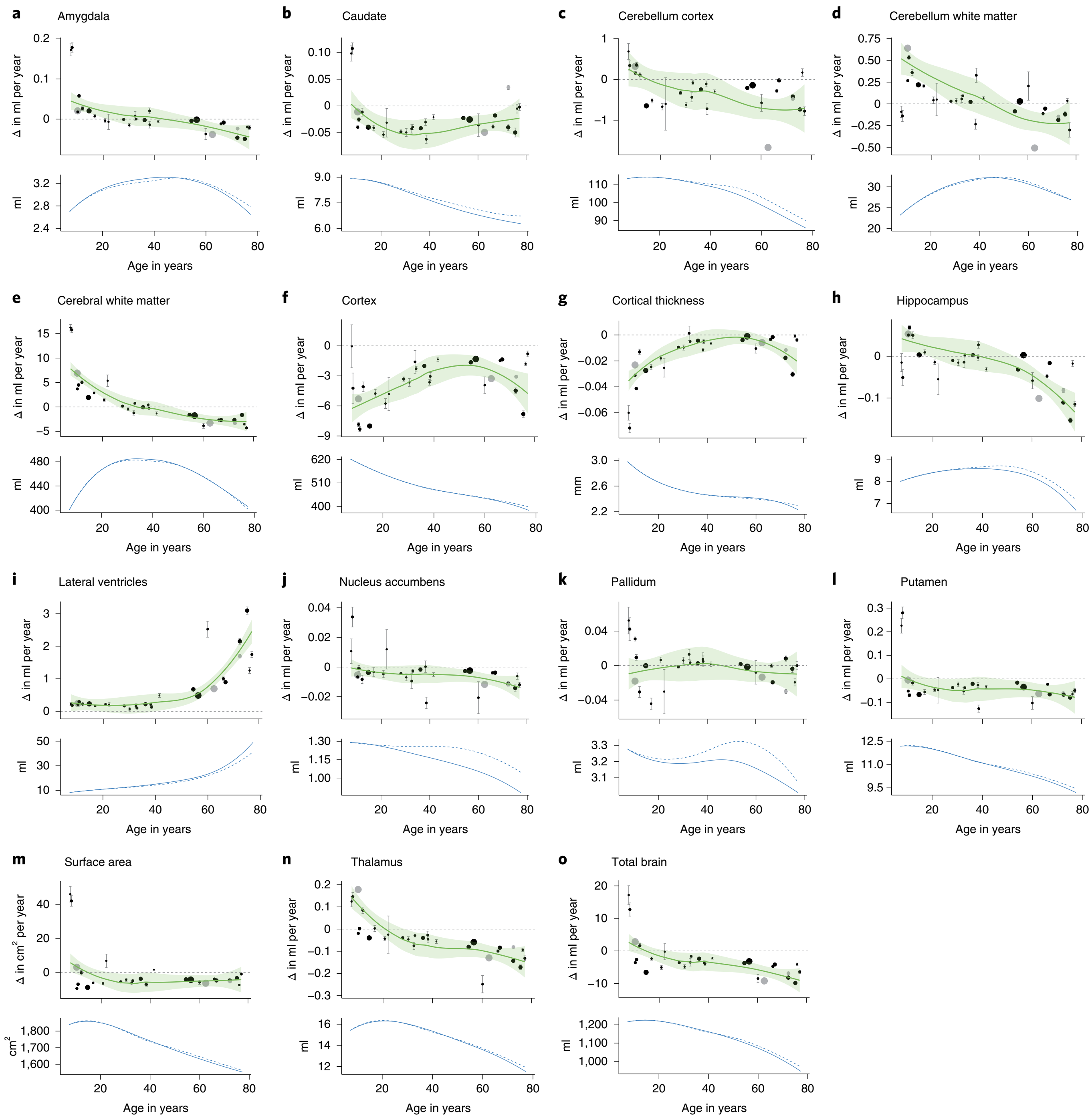

Fig. 2 | Annual rates of change Δ per cohort for each structure. a-o, The estimated trajectories with 95% confidence intervals (in green) are displayed in the top row. Mean values of individual cohorts are displayed as points, with error bars representing standard errors displayed in gray. The size of the points represents the relative size of the cohorts (total sample size $n = 15{,}640$). Means and standard deviations are based on raw data; no covariates were included. Cohorts that were added in phase 2 are displayed in gray. Only cohorts that satisfy $n > 75$ and mean interval >0.5 years are shown. The estimated trajectories of the volumes themselves are displayed in the bottom row, for all individuals (solid line) and for individuals not part of diagnostic groups (dashed line).

and psychological traits (Methods). We found significant genomic overlap ($P < 1.6 \times 10^{-4}$) with genetic variants associated with depression[27], schizophrenia[28], cognitive functioning[29], height[30], insomnia[31], body mass index (BMI)[30] and ever-smoking[32]. Despite significant pleiotropy between rates of change and these traits, we did not find evidence for concordance or discordance of effects (Fig. 5 and Supplementary Fig. 5). For comparison, we computed the genomic overlap between cross-sectional volumes and these phenotypes using the same method. In general, cross-sectional volumes showed overlap for the same traits and several others. Of note, there was also little overlap between the summary statistics for the longitudinal brain measures and summary statistics for the corresponding volumes, based on cross-sectional data. This implies that, despite the fact that both cross-sectional brain volume and rates of changes

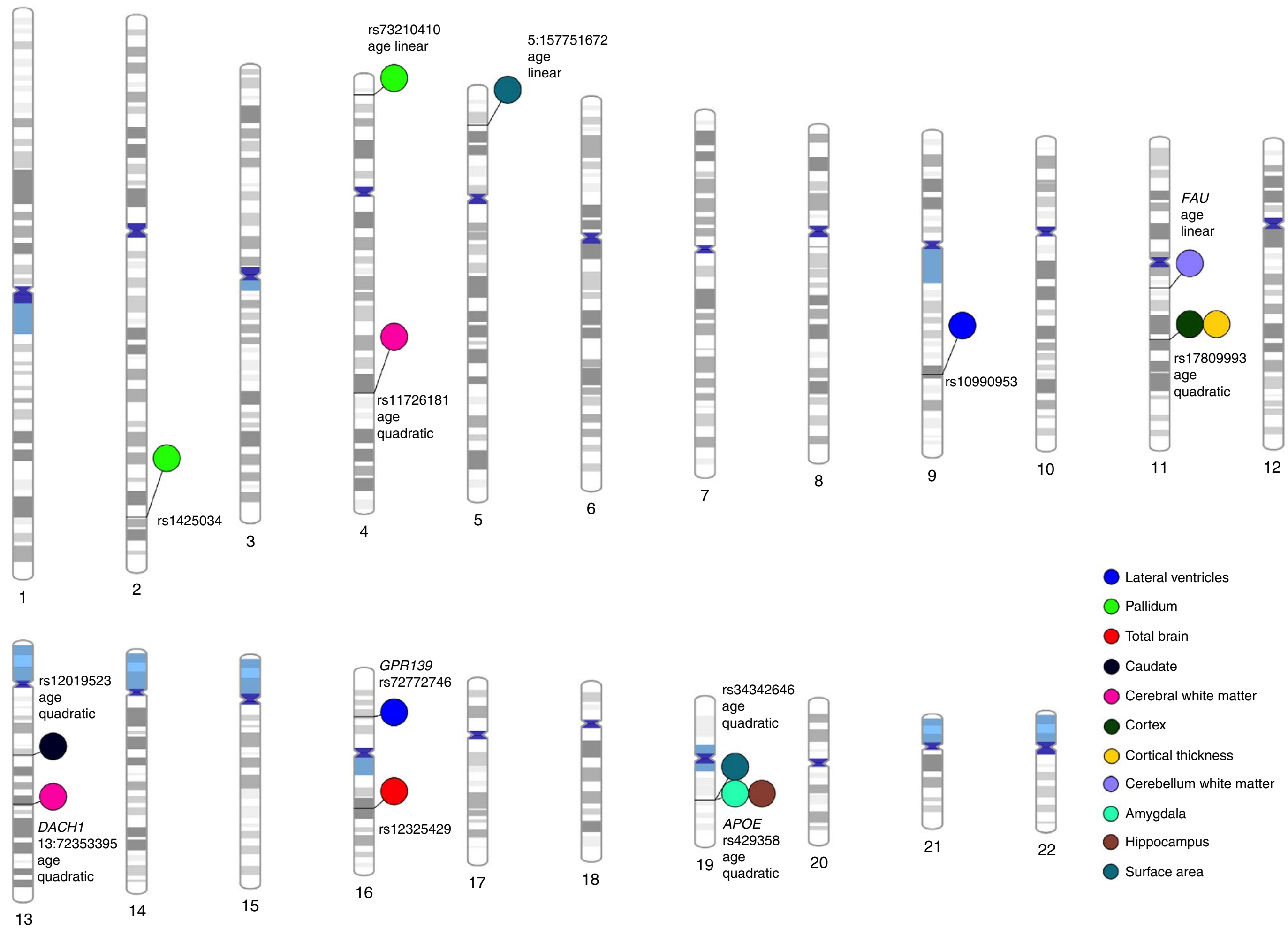

Fig. 3 | Genetic effects on rates of brain changes throughout the lifespan. Genome-wide significant SNPs and genes with effects on brain changes at their respective loci across the human genome, from phase 2 (total $n = 15{,}100$). This plot was created using PhenoGram (http://visualization.ritchielab.org).

are associated with traits such as schizophrenia or cognitive functioning, these associations are likely not driven by the same genomic locations. Additionally, there was little overlap in the genetic loci associated with the longitudinal brain measures and intracranial volume at baseline, indicating that overall head size did not drive our findings (Fig. 5).

Follow-up analyses: gene expression across the lifespan

We determined mRNA expression for genome-wide significant genes and genes associated with genome-wide significant SNPs (Supplementary Tables 5, 7, 9 and 11) in 54 tissue types and in both the developing and adult human brain (Methods). For the prioritized genes, a gene expression heat map was created, based on GTEx version 8 RNA sequencing data[33]. This revealed considerable expression levels across several brain tissues for the following genes: *APOE*, *CAB39L*, *FAU*, *NECTIN2* (alias *PVRL2*) and *SORCS2*, the latter showing higher expression in brain tissue compared to all other tissue types (Supplementary Fig. 6A). These genes show different expression patterns across the lifespan in the BrainSpan data[34]. *DACH1* shows highest expression during early prenatal stages (8–9 post-conception weeks) compared to postnatal stages. Several genes demonstrate stable high expression levels throughout development and across the lifespan (*APOE*, *CAB39L*, *FAU* and *NECTIN2* (alias *PVRL2*)). *CDH8* shows lower expression in the early prenatal stages and higher expression later in life (Supplementary Fig. 6b).

Follow-up analyses: phenome-wide associations

For the prioritized SNPs and genes (Supplementary Tables 5, 7, 9 and 11), exploratory pheWAS (that is, 'phenome-wide') analysis was performed to systematically analyze many phenotypes for association with the genotype and individual genes (Supplementary Table 17). pheWAS was performed using publicly available data from the GWAS Atlas[32] (https://atlas.ctglab.nl). Gene associations of *DACH1*, *GPR139* and *SORCS2* showed pleiotropic effects mainly in the metabolic domain—for example, with estimated glomerular filtration rate and BMI (Supplementary Table 17 and Supplementary Fig. 7). *SORCS2* and *CDH8* also showed significant associations with psychiatric and cognitive traits. Both *APOE* and *NECTIN2* showed strongest associations with AD, cholesterol and lipids (Supplementary Table 17 and Supplementary Fig. 7).

Sensitivity analyses

We repeated the SNP and gene analyses in various subgroups: (1) by adding four cohorts of non-European or mixed ancestry ($n = 540$; total $n = 15{,}640$); (2) by omitting cohorts that did not meet a minimum sample size criterion ($n > 75$) or a minimum scanning interval (>0.5 years), leaving $n = 14{,}601$; (3) by excluding diagnostic groups in each cohort, leaving $n = 13{,}390$; and (4) by including a covariate adjusting for disease status (Supplementary Tables 18 and 19). In SNP-based and gene-based analyses, effect sizes of SNPs were very similar in all subgroups, suggesting that our results are also applicable for individuals of non-European ancestry (with the

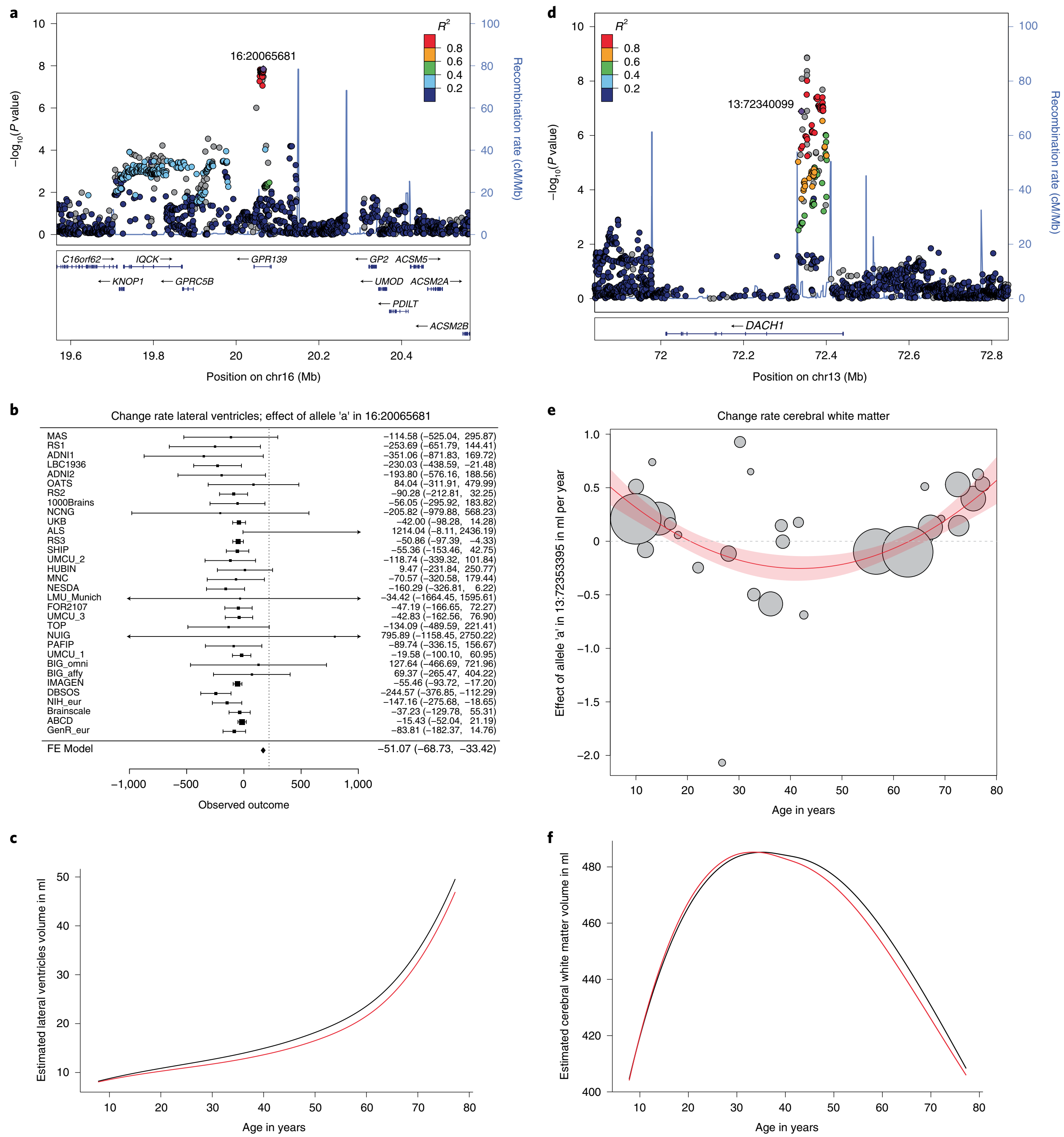

Fig. 4 | Summary of findings for two top SNPs. Shown here is a summary of findings for a top SNP of an age-independent effect (rs72772746; intron to *GPR139*; associated with rate of change of lateral ventricle volume; left column) and a top SNP of an age-dependent effect (13:72353395; intron to *DACH1*; associated with rate of change in cerebral white matter volume; right column). Displayed are the locus plots (**a** and **d**), forest plot (**b**; total $n = 14,593$; means and 95% confidence intervals are displayed for each cohort; confidence intervals that are outside the axis of the plot are marked with an arrow) and plot of meta-regression (**e**; total $n = 13,864$; center of the circles represent the effect size of the tested allele for each cohort; radius of the circles are proportional to sample size) and inferred lifespan trajectories for carriers (in red) and non-carriers (in black) of the effect allele (**c** and **f**). Note that 13:72353395 was not in the reference dataset containing LD structure; the displayed LD structure is based on 13:7234009, $R^2 = 0.87$ with the top SNP.

caveat that the non-European subgroup was rather small) and were not driven by the smaller cohorts. Findings were also similar in the healthy subgroup and when correcting for disease status, with one notable exception: the association between *APOE* and rate of volume change in hippocampus and amygdala, with increasing influence of the top SNP with age, was no longer present after correcting for disease (see Supplementary Table 1 for diagnoses). This suggests that these *APOE* findings were, in part, driven by the

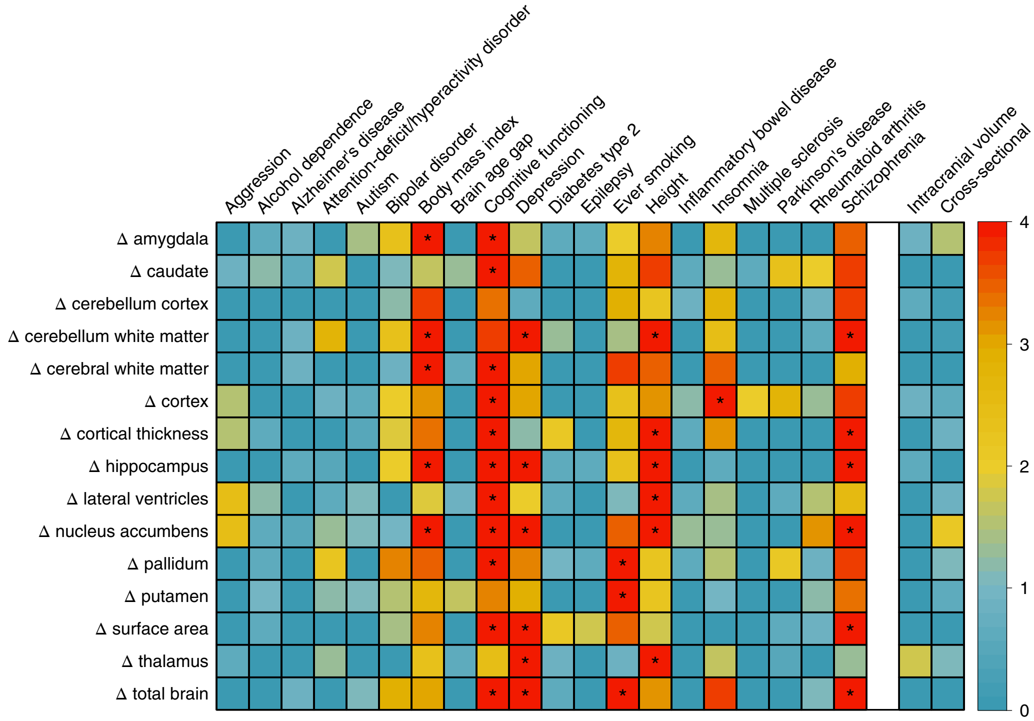

Fig. 5 | Genetic overlap with other phenotypes. *P* values for pleiotropy between change rates of structural brain measures (rows, indicated by Δ for change rate) and neuropsychiatric, disease-related and psychological traits (columns on the left). *P* values for pleiotropy between change rates of structural brain measures and head size (intracranial volume) and the cross-sectional brain measure are displayed on the right. The color legend is displayed on the right, indicating the $-\log_{10} P$ value. Significant overlap ($P < 1.6 \times 10^{-4}$; obtained through permutation testing, two-sided, Bonferroni-corrected) is marked with *. *P* values underlying this figure can be found in Supplementary Table 16.

presence of patients in the cohorts and could, therefore, be explained either by disease-related genes that also influence rates of change or by brain changes occurring as a consequence of the disease.

Given that our main analyses included patients, and iSECA analyses showed several associations with disease, we repeated iSECA analyses excluding diagnostic groups in each cohort. These analyses implicate the same traits, associated with largely the same rates of change of brain measures (Supplementary Fig. 5).

Discussion

Here we present, to our knowledge, the first GWAS investigating influences of common genetic variants on brain structural changes in over 15,000 individuals covering the lifespan. The longitudinal design of our study, combined with the large age range assessed, provides a flexible framework to detect age-independent and age-dependent effects of genetic variants on rates of structural brain changes. We identified genetic variants for structural brain changes between 4 and 99 years of age. Some of these were independent of age, showing effects that were stable throughout life in terms of strength and direction, suggesting that these genetic variants are equally crucial for early brain development as for brain aging. In addition, we identified age-dependent genetic variants, suggesting that some genetic variants are predominantly associated with brain development, whereas others are mainly associated with brain aging.

Among our top findings is the *APOE* gene, a major risk factor for AD[23], and specifically a missense variant in that gene, which influences rates of change in amygdala and hippocampus volume with varying and differential effects across the lifespan, with probably most pronounced effects in those affected with brain disorders. Although most of the additional genetic loci identified here have not previously been associated with any brain-plasticity-related phenotypes, several others were also linked to brain disorders, including psychiatric disorders (for example, *GPR139* and *CDH8*) and neurodegenerative disorders (for example, *NECTIN2*). Notably, *DACH1* and *NECTIN2* show increased expression during early development, whereas other genes' brain expression patterns are most pronounced during adulthood (for example, *APOE* and *CDH8*), suggesting that these genes may exert specific effects during different developmental periods.

Gene set analysis also implies a role for both developmental and neurodegenerative processes. We found a gene set involved in 'neural nucleus development' that influenced rates of change in cerebellar white matter. Other closely related GO terms, 'development of the substantia nigra and midbrain nuclei', were associated with rates of change of cerebral white matter volume and surface area. These all implicate the biological process of progression of a neural nucleus, a compact cluster of neurons in the brain, from its initial condition or formation to its mature state. This would also suggest that we observed the influence of genes involved in early developmental mechanisms of (subcortical) nuclei on cortical changes later in life. It is unclear whether this is a direct effect of these gene sets on cortical changes in adulthood or the consequence of these early developmental pathways. In addition, we found several gene sets interacting with tau protein associated with rate of change in caudate volume and a gene set associated with rate of change in surface area that implicates phorbol 13-acetate 12-myristate, an activator of PKC[25]. PKC is a family of enzymes whose members transduce a large variety of cellular signals and plays a key role in controlling the balance between cell survival and cell death. Its loss of function is generally associated with cancer, whereas its enhanced activity is associated with neurodegeneration. PKC both directly phosphorylates tau and indirectly causes the de-phosphorylation of tau and has been suggested to play a key role in the pathology of AD[35]. Together, these results suggest involvement of genes in aging and neurodegeneration.

At the global, genome-wide level, we found significant genomic overlap between genetic variants associated with rate of change with genetic variants associated with depression, schizophrenia, cognitive functioning, insomnia, height, BMI and ever-smoking. Several of these traits, such as schizophrenia, smoking, cognitive functioning and BMI, have been associated with longitudinal brain structural changes[5,36–38]. The global overlap coincides with findings at the individual gene level: several of the identified genetic variants and genes were linked to metabolic processes (*APOE*, *DACH1*, *GPR139* and *NECTIN2*), cognitive functioning (*CDH8*), psychiatric traits (*GPR139*, *SORCS2* and *CDH8*) and AD (*NECTIN2* and *APOE*), as apparent from the pheWAS results. Despite the pleiotropic effects, concordance of effects was generally null. This is not surprising, as rate-of-change measures for brain structures are not constant and often switch sign over the course of the lifespan[1,39], whereas the GWAS for other traits assume stability of both the phenotype and the genetic influences on the phenotype over time. As such, concordance and discordance of effects would not be expected.

The advantage of longitudinal analyses is that each individual acts as their own control, allowing us to separate the genetic effects on volumes in cross-sectional studies from those on the rates of change[14]. Indeed, we found little overlap between the two: top genes identified in the GWAS on cross-sectional brain structure[26,40–42] generally did not overlap with the top genes for the corresponding rates of change. Longitudinal analyses have long been shown to provide different information from cross-sectional approaches. On a phenotypic level, aging patterns of the hippocampus show different results in cross-sectional studies than in longitudinal studies[43]. On a genetic level, a study that included a within-sample SNP-by-age interaction in the Alzheimer's Disease Neuroimaging Initiative (ADNI) cohort showed that the power to detect genetic associations was larger for a longitudinal design than for a cross-sectional analysis[44]. Of note, that study also identified rs429358 in *APOE* as being associated with longitudinal hippocampal and amygdala volume change in older age (the ADNI cohort is also included in the current study). Through our meta-regression approach, we now show this variant to exert an effect across the lifespan, with the risk variant for AD causing faster increases in childhood for amygdala volume and faster volume reductions for both amygdala and hippocampus later in life.

Given the dynamics of brain structural changes during the lifespan, we investigated both age-independent and age-dependent genetic effects. The age-independent effects can be interpreted as neurodevelopmental influences that also affect brain structure at older ages[45,46], whereas the age-dependent effects can be interpreted as possible changing effects of genes or gene expression during life[16]. The genome-wide meta-regression approach employed here may enable future GWASs for other phenotypes that change over the human lifespan.

We chose to analyze longitudinal changes for 15 separate brain structures, because we observed generally low correlations between these phenotypic changes. This approach allowed us to find brain-structure-specific associations. However, several longitudinal studies have described phenotypic correlations between structural changes[39,47,48]; combining several phenotypes could, thus, be an alternative approach to identify genetic variants that exert a global effect. Of note, cohort and age are intertwined in our meta-regression analysis. Although the cohorts analyzed in this study together cover the full lifespan, there is relatively little age overlap between them; therefore, we cannot be sure that differences between cohorts can be exclusively attributed to age. Mega-analysis would circumvent this problem, but this was not feasible in practice. Moreover, we imposed the same stringent criteria of genome-wide significance for the age-independent meta-analysis and age-dependent meta-regression, which renders chance findings equally unlikely in either type of analysis. In addition, residual heterogeneity for the top findings was generally small. That said, our sample size is still relatively modest for GWAS purposes, and replication in larger samples and inclusion of other ancestries is needed once more longitudinal data become available.

How exactly variation in these genes affects brain changes in health and disease cannot be answered based on GWASs. To this end, our findings may direct future studies into brain development and aging and prevention and treatment of brain disorders. For example, biological pathways that guide neural nucleus development in the fetal subcortical brain may be particularly relevant to the cerebral white matter growth and cortical thinning that takes place during childhood and adolescence. Neurodegenerative disorders might be better understood when genetic variants that influence brain atrophy over time are identified, compared with identification of static genetic differences. In conclusion, our study shows that our genetic architecture is associated with the dynamics of human brain structure throughout life.

Online content

Any methods, additional references, Nature Research reporting summaries, source data, extended data, supplementary information, acknowledgements, peer review information; details of author contributions and competing interests; and statements of data and code availability are available at https://doi.org/10.1038/s41593-022-01042-4.

Received: 28 August 2020; Accepted: 28 February 2022;
Published online: 5 April 2022

References

1. Hedman, A. M., van Haren, N. E., Schnack, H. G., Kahn, R. S. & Hulshoff Pol, H. E. Human brain changes across the life span: a review of 56 longitudinal magnetic resonance imaging studies. *Hum. Brain Mapp.* **33**, 1987–2002 (2012).
2. Giedd, J. N. et al. Brain development during childhood and adolescence: a longitudinal MRI study. *Nat. Neurosci.* **2**, 861–863 (1999).
3. Raz, N. et al. Regional brain changes in aging healthy adults: general trends, individual differences and modifiers. *Cereb. Cortex* **15**, 1676–1689 (2005).
4. Ramsden, S. et al. Verbal and non-verbal intelligence changes in the teenage brain. *Nature* **0**, 6–10 (2011).
5. Schnack, H. G. et al. Changes in thickness and surface area of the human cortex and their relationship with intelligence. *Cereb. Cortex* **25**, 1608–1617 (2015).
6. Shaw, P. et al. Development of cortical asymmetry in typically developing children and its disruptionin attention-deficit/hyperactivity disorder. *Arch. Gen. Psychiatry* **66**, 888–896 (2009).
7. DeLisi, L. E., Sakuma, M., Maurizio, A. M., Relja, M. & Hoff, A. L. Cerebral ventricular change over the first 10 years after the onset of schizophrenia. *Psychiatry Res.* **130**, 57–70 (2004).
8. Reiter, K. et al. Five-year longitudinal brain volume change in healthy elders at genetic risk for Alzheimer's disease. *J. Alzheimers Dis.* **55**, 1363–1377 (2017).
9. Eshaghi, A. et al. Deep gray matter volume loss drives disability worsening in multiple sclerosis. *Ann. Neurol.* **83**, 210–222 (2018).
10. Brouwer, R. M. et al. Heritability of brain volume change and its relation to intelligence. *Neuroimage* **100**, 676–683 (2014).
11. Brans, R. G. H. et al. Heritability of changes in brain volume over time i n twin pairs discordant for schizophrenia. *Arch. Gen. Psychiatry* **65**, 1259–1268 (2008).
12. Kaufmann, T. et al. Common brain disorders are associated with heritable patterns of apparent aging of the brain. *Nat. Neurosci.* **22**, 1617–1623 (2019).
13. Thompson, P. M. et al. ENIGMA and global neuroscience: a decade of large-scale studies of the brain in health and disease across more than 40 countries. *Transl. Psychiatry* **10**, 1–28 (2020).
14. Brouwer, R. M. et al. Genetic influences on individual differences in longitudinal changes in global and subcortical brain volumes: results of the ENIGMA plasticity working group. *Hum. Brain Mapp.* **38**, 4444–4458 (2017).
15. Szekely, E. et al. Genetic associations with childhood brain growth, defined in two longitudinal cohorts. *Genet. Epidemiol.* **42**, 405–414 (2018).
16. Kang, H. et al. Spatio-temporal transcriptome of the human brain. *Nature* **478**, 483–489 (2011).
17. Fletcher, S. C. How (not) to measure replication. *Eur. J. Philos. Sci.* **11**, 57 (2021).
18. Nøhr, A. C. et al. Identification of a novel scaffold for a small molecule GPR139 receptor agonist. *Sci. Rep.* **9**, 3802 (2019).

19. Süsens, U., Hermans-Borgmeyer, I., Urny, J. & Schaller, H. C. Characterisation and differential expression of two very closely related G-protein-coupled receptors, GPR139 and GPR142, in mouse tissue and during mouse development. *Neuropharmacology* **50**, 512–520 (2006).
20. Dao, M., Stoveken, H. M., Cao, Y. & Martemyanov, K. A. The role of orphan receptor GPR139 in neuropsychiatric behavior. *Neuropsychopharmacology* **47**, 902–913 (2021).
21. Pagnamenta, A. T. et al. Rare familial 16q21 microdeletions under a linkage peak implicate cadherin 8 (*CDH8*) in susceptibility to autism and learning disability. *J. Med. Genet.* **48**, 48–54 (2011).
22. Castiglioni, V. et al. Dynamic and cell-specific DACH1 expression in human neocortical and striatal development. *Cereb. Cortex* **29**, 2115–2124 (2019).
23. Wolfe, C. M., Fitz, N. F., Nam, K. N., Lefterov, I. & Koldamova, R. The role of APOE and TREM2 in Alzheimer's disease—current understanding and perspectives. *Int. J. Mol. Sci.* **20**, 65–70 (2019).
24. Hauser, P. S., Narayanaswami, V. & Ryan, R. O. Apolipoprotein E: from lipid transport to neurobiology. *Prog. Lipid Res.* **50**, 62–74 (2011).
25. Steinberg, S. F. Structural basis of protein kinase C isoform function. *Physiol. Rev.* **88**, 1341–1378 (2008).
26. Hibar, D. P. et al. Novel genetic loci associated with hippocampal volume. *Nat. Commun.* **8**, 13624 (2017).
27. Howard, D. M. et al. Genome-wide meta-analysis of depression identifies 102 independent variants and highlights the importance of the prefrontal brain regions. *Nat. Neurosci.* **22**, 343–352 (2019).
28. Psychiatric Genomics Consortium. Biological insights from 108 schizophrenia-associated genetic loci. *Nature* **511**, 421–427 (2014).
29. Savage, J. E. et al. Genome-wide association meta-analysis in 269,867 individuals identifies new genetic and functional links to intelligence. *Nat. Genet.* **50**, 912–919 (2018).
30. Yengo, L. et al. Meta-analysis of genome-wide association studies for height and body mass index in ~700 000 individuals of European ancestry. *Hum. Mol. Genet.* **27**, 3641–3649 (2018).
31. Jansen, P. R. et al. Genome-wide analysis of insomnia in 1,331,010 individuals identifies new risk loci and functional pathways. *Nat. Genet.* **51**, 394–403 (2019).
32. Watanabe, K. et al. A global overview of pleiotropy and genetic architecture in complex traits. *Nat. Genet.* **51**, 1339–1348 (2019).
33. The GTEx Consortium. The Genotype-Tissue Expression (GTEx) pilot analysis: multitissue gene regulation in humans. *Science* **348**, 648–660 (2015).
34. Miller, J. A. et al. Transcriptional landscape of the prenatal human brain. *Nature* **508**, 199–206 (2014).
35. Callender, J. A. & Newton, A. C. Conventional protein kinase C in the brain: 40 years later. *Neuronal Signal.* **1**, NS20160005 (2017).
36. Bobb, J. F., Schwartz, B. S., Davatzikos, C. & Caffo, B. Cross-sectional and longitudinal association of body mass index and brain volume. *Hum. Brain Mapp.* **35**, 75–88 (2014).
37. Kim, R. E. et al. Lifestyle-dependent brain change: a longitudinal cohort MRI study. *Neurobiol. Aging* **69**, 48–57 (2018).
38. Hulshoff Pol, H. E. & Kahn, R. S. What happens after the first episode? A review of progressive brain changes in chronically ill patients with schizophrenia. *Schizophr. Bull.* **34**, 354–366 (2008).
39. Fjell, A. M. et al. The genetic organization of longitudinal subcortical volumetric change is stable throughout the lifespan. *eLife* **10**, e66466 (2021).
40. Elliott, L. T. et al. Genome-wide association studies of brain imaging phenotypes in UK Biobank. *Nature* **562**, 210–216 (2018).
41. Satizabal, C. L. et al. Genetic architecture of subcortical brain structures in 38,851 individuals. *Nat. Genet.* **51**, 1624–1636 (2019).
42. Grasby, K. L. et al. The genetic architecture of the human cerebral cortex. *Science* **367**, eaay6690 (2020).
43. Pfefferbaum, A. & Sullivan, E. V. Cross-sectional versus longitudinal estimates of age-related changes in the adult brain: overlaps and discrepancies. *Neurobiol. Aging* **36**, 2563–2567 (2015).
44. Xu, Z., Shen, X., Pan, W. & Alzheimer's Disease Neuroimaging Initiative. Longitudinal analysis is more powerful than cross-sectional analysis in detecting genetic association with neuroimaging phenotypes. *PLoS ONE* **9**, e102312 (2014).
45. Fjell, A. M. et al. Development and aging of cortical thickness correspond to genetic organization patterns. *Proc. Natl Acad. Sci. USA* **112**, 15462–7 (2015).
46. Walhovd, K. B. et al. Neurodevelopmental origins of lifespan changes in brain and cognition. *Proc. Natl Acad. Sci. USA* **113**, 9357–9362 (2016).
47. Sullivan, E. V. differential rates of regional brain change in callosal and ventricular size: a 4-year longitudinal MRI study of elderly men. *Cereb. Cortex* **12**, 438–445 (2002).
48. Storsve, A. B. et al. Differential longitudinal changes in cortical thickness, surface area and volume across the adult life span: regions of accelerating and decelerating change. *J. Neurosci.* **34**, 8488–8498 (2014).

Rachel M. Brouwer[1,2]✉, Marieke Klein[1,3,4,5], Katrina L. Grasby[6], Hugo G. Schnack[1,7], Neda Jahanshad[8], Jalmar Teeuw[1], Sophia I. Thomopoulos[8], Emma Sprooten[9], Carol E. Franz[10], Nitin Gogtay[11], William S. Kremen[10,12], Matthew S. Panizzon[10], Loes M. Olde Loohuis[13], Christopher D. Whelan[14], Moji Aghajani[15,16], Clara Alloza[17], Dag Alnæs[18,19], Eric Artiges[20], Rosa Ayesa-Arriola[21,22,23], Gareth J. Barker[24], Mark E. Bastin[25,26,27], Elisabet Blok[28], Erlend Bøen[29], Isabella A. Breukelaar[30], Joanna K. Bright[8], Elizabeth E. L. Buimer[1], Robin Bülow[31], Dara M. Cannon[32], Simone Ciufolini[33], Nicolas A. Crossley[33,34], Christienne G. Damatac[9], Paola Dazzan[35], Casper L. de Mol[36], Sonja M. C. de Zwarte[1], Sylvane Desrivières[37], Covadonga M. Díaz-Caneja[17], Nhat Trung Doan[18], Katharina Dohm[38], Juliane H. Fröhner[39], Janik Goltermann[38], Antoine Grigis[40], Dominik Grotegerd[38], Laura K. M. Han[15], Mathew A. Harris[25], Catharina A. Hartman[41], Sarah J. Heany[42], Walter Heindel[43], Dirk J. Heslenfeld[44], Sarah Hohmann[45], Bernd Ittermann[46], Philip R. Jansen[2,28,47], Joost Janssen[17], Tianye Jia[48,49], Jiyang Jiang[50], Christiane Jockwitz[51,52], Temmuz Karali[53,54], Daniel Keeser[53,54,55], Martijn G. J. C. Koevoets[1], Rhoshel K. Lenroot[56,57,58], Berend Malchow[59], René C. W. Mandl[1], Vicente Medel[34], Susanne Meinert[38,60], Catherine A. Morgan[61,62], Thomas W. Mühleisen[51,63,64], Leila Nabulsi[32], Nils Opel[38,65], Víctor Ortiz-García de la Foz[21,22,66], Bronwyn J. Overs[58], Marie-Laure Paillère Martinot[20,67], Ronny Redlich[38,68], Tiago Reis Marques[33,69], Jonathan Repple[38], Gloria Roberts[56], Gennady V. Roshchupkin[70,71], Nikita Setiaman[1,28], Elena Shumskaya[4,9], Frederike Stein[72], Gustavo Sudre[73], Shun Takahashi[53,74], Anbupalam Thalamuthu[50], Diana Tordesillas-Gutiérrez[75,76], Aad van der Lugt[71], Neeltje E. M. van Haren[1,28],

Joanna M. Wardlaw[25,77], Wei Wen[50], Henk-Jan Westeneng[78], Katharina Wittfeld[79,80], Alyssa H. Zhu[8], Andre Zugman[81,82], Nicola J. Armstrong[83], Gaia Bonfiglio[2], Janita Bralten[4,5], Shareefa Dalvie[42], Gail Davies[25,84], Marta Di Forti[37], Linda Ding[8], Gary Donohoe[85], Andreas J. Forstner[51,86,87], Javier Gonzalez-Peñas[17], Joao P. O. F. T. Guimaraes[4,9], Georg Homuth[88], Jouke-Jan Hottenga[89], Maria J. Knol[70], John B. J. Kwok[90,91], Stephanie Le Hellard[92,93], Karen A. Mather[50,58], Yuri Milaneschi[15], Derek W. Morris[85], Markus M. Nöthen[87], Sergi Papiol[22,53,94], Marcella Rietschel[95], Marcos L. Santoro[81,82,96], Vidar M. Steen[92,93], Jason L. Stein[97], Fabian Streit[95], Rick M. Tankard[83], Alexander Teumer[98], Dennis van 't Ent[89], Dennis van der Meer[18,19,99], Kristel R. van Eijk[78], Evangelos Vassos[37,100], Javier Vázquez-Bourgon[21,22,23], Stephanie H. Witt[95], the IMAGEN Consortium*, Hieab H. H. Adams[71,101,102], Ingrid Agartz[18,103,104], David Ames[105,106], Katrin Amunts[51,63], Ole A. Andreassen[18,19], Celso Arango[17], Tobias Banaschewski[45], Bernhard T. Baune[107,108,109], Sintia I. Belangero[81,82,96], Arun L. W. Bokde[110], Dorret I. Boomsma[89], Rodrigo A. Bressan[81,82,111], Henry Brodaty[50], Jan K. Buitelaar[9,112], Wiepke Cahn[1,113], Svenja Caspers[51,52], Sven Cichon[51,64,114], Benedicto Crespo-Facorro[22,115], Simon R. Cox[25,116], Udo Dannlowski[38], Torbjørn Elvsåshagen[117,118,119], Thomas Espeseth[120,121], Peter G. Falkai[53], Simon E. Fisher[5,122], Herta Flor[123], Janice M. Fullerton[58,91], Hugh Garavan[124], Penny A. Gowland[125], Hans J. Grabe[79,80], Tim Hahn[38], Andreas Heinz[126], Manon Hillegers[1,28], Jacqueline Hoare[42,127], Pieter J. Hoekstra[128], Mohammad A. Ikram[70], Andrea P. Jackowski[81,82], Andreas Jansen[72,129], Erik G. Jönsson[18,103], Rene S. Kahn[130,131], Tilo Kircher[72], Mayuresh S. Korgaonkar[30,90], Axel Krug[72,132], Herve Lemaitre[133], Ulrik F. Malt[134], Jean-Luc Martinot[20], Colm McDonald[32], Philip B. Mitchell[56], Ryan L. Muetzel[28], Robin M. Murray[33], Frauke Nees[45,123,135], Igor Nenadić[72], Jaap Oosterlaan[136,137], Roel A. Ophoff[13,138], Pedro M. Pan[81,82], Brenda W. J. H. Penninx[15], Luise Poustka[139], Perminder S. Sachdev[50,140], Giovanni A. Salum[82,141,142], Peter R. Schofield[58,91], Gunter Schumann[143,144], Philip Shaw[73,145], Kang Sim[146,147], Michael N. Smolka[148], Dan J. Stein[149], Julian N. Trollor[50,150], Leonard H. van den Berg[78], Jan H. Veldink[78], Henrik Walter[151], Lars T. Westlye[18,19,120], Robert Whelan[152], Tonya White[28,71], Margaret J. Wright[153,154], Sarah E. Medland[155], Barbara Franke[4,5,156,163], Paul M. Thompson[8,163] and Hilleke E. Hulshoff Pol[1,157,163] ✉

[1]Department of Psychiatry, University Medical Center Utrecht Brain Center, Utrecht University, Utrecht, The Netherlands. [2]Department of Complex Trait Genetics, Center for Neurogenomics and Cognitive Research, Amsterdam Neuroscience, VU Amsterdam, Amsterdam, The Netherlands. [3]Department of Psychiatry, University of California, San Diego, La Jolla, CA, USA. [4]Department of Human Genetics, Radboud University Medical Center, Nijmegen, The Netherlands. [5]Donders Institute for Brain, Cognition and Behaviour, Radboud University, Nijmegen, The Netherlands. [6]Psychiatric Genetics, QIMR Berghofer Medical Research Institute, Brisbane, QLD, Australia. [7]Utrecht Institute of Linguistics OTS, Utrecht University, Utrecht, The Netherlands. [8]Imaging Genetics Center, Mark and Mary Stevens Neuroimaging and Informatics Institute, Keck School of Medicine, University of Southern California, Marina del Rey, CA, USA. [9]Department of Cognitive Neuroscience, Donders Institute for Brain, Cognition and Behaviour, Radboud University Medical Center, Nijmegen, The Netherlands. [10]Department of Psychiatry and Center for Behavior Genetics of Aging, University of California, San Diego, La Jolla, CA, USA. [11]American Psychiatric Association, Washington, DC, USA. [12]VA San Diego Center of Excellence for Stress and Mental Health, San Diego, CA, USA. [13]Center for Neurobehavioral Genetics, University of California, Los Angeles, Los Angeles, CA, USA. [14]Biogen Research and Development, Cambridge, MA, USA. [15]Department of Psychiatry, Amsterdam Public Health and Amsterdam Neuroscience, Amsterdam UMC, Vrije Universiteit, Amsterdam, The Netherlands. [16]Institute of Education & Child Studies, Section Forensic Family & Youth Care, Leiden University, Leiden, The Netherlands. [17]Department of Child and Adolescent Psychiatry, Institute of Psychiatry and Mental Health, Hospital General Universitario Gregorio Marañón, IiSGM, CIBERSAM, School of Medicine, Universidad Complutense, Madrid, Spain. [18]NORMENT Centre, University of Oslo, Oslo, Norway. [19]Division of Mental Health and Addiction, Oslo University Hospital, Oslo, Norway. [20]INSERM U1299 Trajectoires Développementales en Psychiatrie, Ecole Normale Supérieure Paris-Saclay, Université Paris Saclay, Université Paris Cité, CNRS UMR 9010; Centre Borelli, Gif-sur-Yvette, France. [21]Valdecilla Biomedical Research Institute (IDIVAL), Marqués de Valdecilla University Hospital (HUMV), School of Medicine, University of Cantabria, Santander, Spain. [22]CIBERSAM, Biomedical Research Network on Mental Health Area, Santander, Spain. [23]Universidad de Cantabria, Santander, Spain. [24]Department of Neuroimaging, Institute of Psychiatry, Psychology & Neuroscience, King's College London, London, UK. [25]Lothian Birth Cohorts group, Department of Psychology, University of Edinburgh,

Edinburgh, UK. [26]Centre for Clinical Brain Sciences, University of Edinburgh, Edinburgh, UK. [27]Edinburgh Imaging, University of Edinburgh, Edinburgh, UK. [28]Department of Child and Adolescent Psychiatry/Psychology, Sophia Children's Hospital, Erasmus University Medical Center Rotterdam, Rotterdam, The Netherlands. [29]Psychosomatic and CL Psychiatry, Oslo University Hospital, Oslo, Norway. [30]Brain Dynamics Centre, Westmead Institute for Medical Research, University of Sydney, Westmead, NSW, Australia. [31]Institute of Diagnostic Radiology and Neuroradiology, University Medicine Greifswald, Greifswald, Germany. [32]Centre for Neuroimaging, Cognition and Genomics (NICOG), Clinical Neuroimaging Laboratory, NCBES Galway Neuroscience Centre, College of Medicine Nursing and Health Sciences, National University of Ireland Galway, Galway, Ireland. [33]Department of Psychosis Studies, Institute of Psychiatry, Psychology and Neuroscience, King's College London, London, UK. [34]Department of Psychiatry, School of Medicine, Pontificia Universidad Católica de Chile, Santiago, Chile. [35]Department of Psychological Medicine, Institute of Psychiatry, Psychology and Neuroscience, King's College London, London, UK. [36]Department of Neurology, Erasmus University Medical Center Rotterdam, Rotterdam, The Netherlands. [37]Social, Genetic and Developmental Psychiatry Centre, Institute of Psychiatry, Psychology & Neuroscience, King's College London, London, UK. [38]Institute for Translational Psychiatry, University of Münster, Münster, Germany. [39]Section of Systems Neuroscience, Department of Psychiatry and Psychotherapy, Technische Universität Dresden, Dresden, Germany. [40]Université Paris-Saclay, CEA, Neurospin, Gif-sur-Yvette, France. [41]University of Groningen, University Medical Center Groningen, Department of Psychiatry, Interdisciplinary Center Psychopathology and Emotion Regulation (ICPE), Groningen, The Netherlands. [42]Department of Psychiatry and Mental Health, University of Cape Town, Cape Town, South Africa. [43]Clinic for Radiology, University Hospital Münster, Münster, Germany. [44]Departments of Experimental and Clinical Psychology, Amsterdam, The Netherlands. [45]Department of Child and Adolescent Psychiatry and Psychotherapy, Central Institute of Mental Health, Medical Faculty Mannheim/Heidelberg University, Mannheim, Germany. [46]Physikalisch-Technische Bundesanstalt, Berlin, Germany. [47]Department of Human Genetics, VUmc, Amsterdam UMC, Amsterdam, The Netherlands. [48]Centre for Population Neuroscience and Precision Medicine (PONS), Institute of Science and Technology for Brain-Inspired Intelligence and MoE Key Laboratory of Computational Neuroscience and Brain-Inspired Intelligence, Fudan University, Shanghai, China. [49]Centre for Population Neuroscience and Precision Medicine (PONS), Institute of Psychiatry, Psychology and Neuroscience, SGDP Centre, King's College London, London, UK. [50]Centre for Healthy Brain Ageing (CHeBA), Discipline of Psychiatry and Mental Health, University of New South Wales, Sydney, NSW, Australia. [51]Institute of Neuroscience and Medicine (INM-1), Research Centre Jülich, Jülich, Germany. [52]Institute for Anatomy I, Medical Faculty & University Hospital Düsseldorf, Heinrich Heine University, Düsseldorf, Germany. [53]Department of Psychiatry and Psychotherapy, University Hospital LMU, Munich, Germany. [54]NeuroImaging Core Unit Munich (NICUM), University Hospital LMU, Munich, Germany. [55]Munich Center for Neurosciences (MCN) – Brain & Mind, Planegg-Martinsried, Germany. [56]School of Psychiatry, University of New South Wales, Sydney, NSW, Australia. [57]School of Psychiatry and Behavioral Sciences, School of Medicine, University of New Mexico, Albuquerque, NM, USA. [58]Neuroscience Research Australia, Sydney, NSW, Australia. [59]Department of Psychiatry and Psychotherapy, University Medical Center Göttingen, Göttingen, Germany. [60]Institute for Translational Neuroscience, University of Münster, Münster, Germany. [61]School of Psychology and Centre for Brain Research, University of Auckland, Auckland, New Zealand. [62]Brain Research New Zealand - Rangahau Roro Aotearoa, Auckland, New Zealand. [63]Cécile and Oskar Vogt Institute for Brain Research, Medical Faculty, University Hospital Düsseldorf, Heinrich Heine University Düsseldorf, Düsseldorf, Germany. [64]Department of Biomedicine, University of Basel, Basel, Switzerland. [65]Department of Psychiatry, Jena University Hospital/Friedrich-Schiller-University Jena, Jena, Germany. [66]Neuroimaging Unit, Technological Facilities, Valdecilla Biomedical Research Institute IDIVAL, Santander, Spain. [67]APHP, Sorbonne Université, Pitie-Salpetriere Hospital, Department of Child and Adolescent Psychiatry, Paris, France. [68]Department of Psychology, University of Halle, Halle, Germany. [69]Psychiatric Imaging Group, MRC London Institute of Medical Sciences (LMS), Imperial College London, London, UK. [70]Department of Epidemiology, Erasmus University Medical Center Rotterdam, Rotterdam, The Netherlands. [71]Department of Radiology & Nuclear Medicine, Erasmus Medical Center, University Medical Center Rotterdam, Rotterdam, The Netherlands. [72]Department of Psychiatry and Psychotherapy, Philipps-University Marburg, Marburg, Germany. [73]Social and Behavioral Research Branch, National Human Genome Research Institute, Bethesda, MD, USA. [74]Department of Neuropsychiatry, Wakayama Medical University, Wakayama, Japan. [75]Department of Radiology, IDIVAL, Marqués de Valdecilla University Hospital, Santander, Spain. [76]Advanced Computing and e-Science, Instituto de Física de Cantabria (UC-CSIC), Santander, Spain. [77]Centre for Clinical Brain Sciences and UK Dementia Research Institute Centre, University of Edinburgh, Edinburgh, UK. [78]Department of Neurology, University Medical Center Utrecht Brain Center, Utrecht University, Utrecht, The Netherlands. [79]German Center for Neurodegenerative Diseases (DZNE), Site Rostock/Greifswald, Greifswald, Germany. [80]Department of Psychiatry and Psychotherapy, University Medicine Greifswald, Greifswald, Germany. [81]Laboratory of Integrative Neuroscience (LiNC), Department of Psychiatry, Universidade Federal de São Paulo (UNIFESP), São Paulo, Brazil. [82]National Institute of Developmental Psychiatry for Children and Adolescents (INPD), CNPq, São Paulo, Brazil. [83]Mathematics and Statistics, Curtin University, Perth, WA, Australia. [84]Department of Psychology, University of Edinburgh, Edinburgh, UK. [85]Centre for Neuroimaging, Cognition and Genomics (NICOG), School of Psychology and Discipline of Biochemistry, National University of Ireland Galway, Galway, Ireland. [86]Centre for Human Genetics, Philipps-University Marburg, Marburg, Germany. [87]Institute of Human Genetics, University of Bonn, School of Medicine & University Hospital Bonn, Bonn, Germany. [88]Interfaculty Institute for Genetics and Functional Genomics, University Medicine Greifswald, Greifswald, Germany. [89]Netherlands Twin Register, Department of Biological Psychology, Vrije Universiteit, Amsterdam, The Netherlands. [90]Faculty of Medicine and Health, University of Sydney, Sydney, NSW, Australia. [91]School of Medical Sciences, University of New South Wales, Sydney, NSW, Australia. [92]NORMENT Centre of Excellence, Department of Clinical Science, University of Bergen, Bergen, Norway. [93]Dr. Einar Martens Research Group for Biological Psychiatry, Department of Medical Genetics, Haukeland University Hospital, Bergen, Norway. [94]Institute of Psychiatric Phenomics and Genomics (IPPG), University Hospital LMU, Munich, Germany. [95]Department of Genetic Epidemiology, Central Institute of Mental Health, Medical Faculty Mannheim, Heidelberg University, Mannheim, Germany. [96]Department of Morphology and Genetics, Universidade Federal de São Paulo (UNIFESP), São Paulo, Brazil. [97]Department of Genetics & UNC Neuroscience Center, University of North Carolina at Chapel Hill, Chapel Hill, NC, USA. [98]Institute for Community Medicine, University Medicine Greifswald, Greifswald, Germany. [99]School of Mental Health and Neuroscience, Faculty of Health, Medicine and Life Sciences, Maastricht University, Maastricht, The Netherlands. [100]NIHR Maudsley Biomedical Research Centre, South London and Maudsley NHS Trust, London, UK. [101]Department of Clinical Genetics, Erasmus University Medical Center Rotterdam, Rotterdam, The Netherlands. [102]Latin American Brain Health Institute (BrainLat), Universidad Adolfo Ibanez, Santiago, Chile. [103]Centre for Psychiatry Research, Department of Clinical Neuroscience, Karolinska Institutet, & Stockholm Health Care Services, Stockholm Region, Stockholm, Sweden. [104]Department of Psychiatric Research, Diakonhjemmet Hospital, Oslo, Norway. [105]Academic Unit for Psychiatry of Old Age, University of Melbourne, Parkville, VIC, Australia. [106]National Ageing Research Institute, Parkville, VIC, Australia. [107]Department of Psychiatry, University of Melbourne, Melbourne VIC, Australia. [108]Florey Institute of Neuroscience and Mental Health, University of Melbourne, Melbourne, VIC, Australia. [109]Department of Psychiatry, University of Münster, Münster, Germany. [110]Discipline of Psychiatry and Trinity College Institute of Neuroscience, Trinity College Dublin, Dublin, Ireland. [111]Instituto Ame Sua Mente, São Paulo, Brazil. [112]Karakter Child and Adolescent Psychiatry University Centre, Nijmegen, The Netherlands. [113]Altrecht Science, Altrecht Mental Health Institute, Utrecht, The Netherlands. [114]Institute of Medical Genetics and Pathology, University Hospital Basel, University of Basel, Basel, Switzerland. [115]Department of Psychiatry, Virgen del Rocio University Hospital, School of Medicine, University of Seville, IBIS, Seville, Spain. [116]Scottish Imaging Network, A Platform for Scientific Excellence (SINAPSE) Collaboration, Edinburgh, UK. [117]NORMENT Centre, Oslo University Hospital, Oslo, Norway. [118]Department of Neurology, Oslo University Hospital, Oslo, Norway. [119]Institute of Clinical Medicine, University of Oslo, Oslo, Norway. [120]Department of Psychology, University of Oslo, Oslo, Norway. [121]Bjørknes College, Oslo, Norway. [122]Language and Genetics Department, Max Planck Institute for Psycholinguistics, Nijmegen, The Netherlands.

[123]Department of Cognitive and Clinical Neuroscience, Central Institute of Mental Health, Medical Faculty Mannheim, Heidelberg University, Mannheim, Germany. [124]Department of Psychiatry, University of Vermont, Burlington, VT, USA. [125]Sir Peter Mansfield Imaging Centre, School of Physics and Astronomy, University of Nottingham, Nottingham, UK. [126]Charité Universitätsmedizin Berlin, Berlin, Germany. [127]Faculty of Health, Peninsula Medical School, University of Plymouth, Plymouth, UK. [128]University of Groningen, University Medical Center Groningen, Department of Child and Adolescent Psychiatry & Accare Child Study Center, Groningen, The Netherlands. [129]Core-Facility Brainimaging, Faculty of Medicine, University of Marburg, Marburg, Germany. [130]Department of Psychiatry, Icahn School of Medicine at Mount Sinai, New York, NY, USA. [131]VISN 2 Mental Illness Research, Education & Clinical Center (MIRECC), James J. Peters Department of Veterans Affairs Medical Center, Bronx, NY, USA. [132]Department of Psychiatry and Psychotherapy, University of Bonn, Bonn, Germany. [133]Groupe d'Imagerie Neurofonctionnelle, Institut des Maladies Neurodégénératives, CNRS UMR 5293, Université de Bordeaux, Centre Broca Nouvelle-Aquitaine, Bordeaux, France. [134]Unit for Psychosomatic Medicine and C-L Psychiatry, University of Oslo, Oslo, Norway. [135]Institute of Medical Psychology and Medical Sociology, University Medical Center Schleswig-Holstein, Kiel University, Kiel, Germany. [136]Emma Children's Hospital, Amsterdam UMC, University of Amsterdam, Emma Neuroscience Group, Department of Pediatrics, Amsterdam Reproduction & Development, Amsterdam, The Netherlands. [137]Vrije Universiteit, Clinical Neuropsychology Section, Amsterdam, The Netherlands. [138]Department of Psychiatry, Erasmus Medical Center, Erasmus University, Rotterdam, The Netherlands. [139]Department of Child and Adolescent Psychiatry, University Medical Center Goettingen, Göttingen, Germany. [140]Neuropsychiatric Institute, The Prince of Wales Hospital, Sydney, NSW, Australia. [141]Department of Psychiatry and Legal Medicine, Universidade Federal do Rio Grande do Sul, Porto Alegre, Brazil. [142]Section on Negative Affect and Social Processes, Hospital de Clínicas de Porto Alegre, Porto Alegre, Brazil. [143]Center for Population Neuroscience and Precision Medicine (PONS), Institute for Science and Technology for Brain-inspired Intelligence (ISTBI), Fudan University, Shanghai, China. [144]PONS Centre, Department of Psychiatry and Clinical Neuroscience, CCM, Charite University Medicine, Berlin, Germany. [145]National Institute of Mental Health, National Institutes of Health, Bethesda, MD, USA. [146]West Region, Institute of Mental Health, Singapore, Singapore. [147]Yong Loo Lin School of Medicine, National University of Singapore, Singapore, Singapore. [148]Department of Psychiatry and Neuroimaging Center, Technische Universität Dresden, Dresden, Germany. [149]SAMRC Unit on Risk & Resilience in Mental Disorders, Department of Psychiatry & Neuroscience Institute, University of Cape Town, Cape Town, South Africa. [150]Department of Developmental Disability Neuropsychiatry, Discipline of Psychiatry and Mental Health, University of New South Wales, Sydney, NSW, Australia. [151]Charité Universitätsmedizin Berlin, corporate member of Freie Universität Berlin, Humboldt-Universität zu Berlin, and Berlin Institute for Health, Berlin, Germany. [152]Trinity College Institute of Neuroscience, Trinity College Dublin, Dublin, Ireland. [153]Queensland Brain Institute, University of Queensland, Brisbane, QLD, Australia. [154]Centre for Advanced Imaging, University of Queensland, Brisbane, QLD, Australia. [155]QIMR Berghofer Medical Research Institute, Brisbane, QLD, Australia. [156]Department of Psychiatry, Radboud University Medical Center, Nijmegen, The Netherlands. [157]Department of Psychology, Utrecht University, Utrecht, The Netherlands. [163]These authors contributed equally: Barbara Franke, Paul M. Thompson, Hilleke E. Hulshoff Pol. *A list of authors and their affiliations appears at the end of the paper. ✉e-mail: r.m2.brouwer@vu.nl; h.e.hulshoffpol@uu.nl

the IMAGEN Consortium

Tobias Banaschewski[45], Gareth J. Barker[24], Arun L. W. Bokde[110], Sylvane Desrivières[37], Herta Flor[123], Antoine Grigis[40], Hugh Garavan[124], Penny A. Gowland[125], Andreas Heinz[126], Rüdiger Brühl[158], Jean-Luc Martinot[20], Marie-Laure Paillère Martinot[20,67], Eric Artiges[20], Frauke Nees[45,123,135], Dimitri Papadopoulos Orfanos[159], Herve Lemaitre[133], Tomáš Paus[160,161], Luise Poustka[139], Sarah Hohmann[45], Sabina Millenet[162], Juliane H. Fröhner[39], Michael N. Smolka[148], Henrik Walter[151], Robert Whelan[152] and Gunter Schumann[143,144]

[158]Physikalisch-Technische Bundesanstalt (PTB), Braunschweig and Berlin, Berlin, Germany. [159]Université Paris-Saclay, CEA, Neurospin, Gif-sur-Yvette, France. [160]Department of Psychiatry, Faculty of Medicine and Centre Hospitalier Universitaire Sainte-Justine, University of Montreal, Montreal, QB, Canada. [161]Departments of Psychiatry and Psychology, University of Toronto, Toronto, ON, Canada. [162]Department of Child and Adolescent Psychiatry and Psychotherapy, Central Institute of Mental Health, Medical Faculty Mannheim, Heidelberg University, Mannheim, Germany.

Methods

Ethical approval. All participants gave written informed consent, and all participating sites obtained approval from local research ethics committees and institutional review boards. Ethics approval for meta-analyses within the ENIGMA consortium was granted by the QIMR Berghofer Medical Research Institute Human Research Ethics Committee in Australia (approval P2204).

Inclusion criteria. Cohorts that had longitudinal MRI data of the brain and genotyped data extracted from blood or saliva available were invited to participate, irrespective of disease status and age. Patients were not excluded, as aberrant brain trajectories are often observed, and we hypothesized that genetic risk for disease may be associated with genetic influences on rates of change. We included cohorts that had a preferred sample size of at least 75 individuals and a follow-up duration (for repeated MRI scans) of at least 6 months. After quality control of individuals' imaging and genotyping data, not all cohorts could meet these criteria. In total, we included 15,640 individuals aged 4–99 years (49% female and 14% patients). See Extended Data Fig. 1 and Supplementary Table 1 for further description of the cohorts.

Longitudinal imaging. Eight global brain measures (total brain including cerebellum and excluding brainstem, surface area measured at the gray–white matter boundary, average cortical thickness, total lateral ventricle volume and cortical and cerebellar gray and white matter volume) and seven subcortical structures (thalamus, caudate, putamen, pallidum, hippocampus, amygdala and nucleus accumbens) were extracted from the FreeSurfer processing pipeline[49–51] (see Supplementary Table 2 for details per cohort). We chose these measures based on the fact that they show generally high test–retest reliability for cross-sectional measures[52–54], thereby selecting those measures that would have sufficient signal to noise in change measures. Image processing and quality control were performed at the level of the cohorts, following harmonized protocols (http://enigma.ini.usc.edu/protocols/imaging-protocols/), which included visual inspection of the segmentation. Annual rates of change were computed in each individual for each phenotype by subtracting baseline brain measures from follow-up measures and dividing by the number of years of follow-up duration. We chose not to correct for overall head size in the main analysis. Although it is common practice to correct for intracranial volume when investigating cross-sectional brain volumes[55], the associations between intracranial volume and brain changes over time are small (Extended Data Fig. 2), and GWAS findings are very similar with and without correction (Supplementary Note and Supplementary Fig. 8). Distributions of baseline and follow-up measures—as well as annual rates of changes—were visually inspected, and change rates were centrally compared for consistency.

Longitudinal trajectories of brain structure rates of change were estimated by applying locally, cohort-size weighted, estimated scatterplot smoothing with a Gaussian kernel, local polynomials of degree 2 and a span of 1 (LOWESS[56]) implemented in R[57]. Integrating these trajectories and then fitting these to the baseline values of the phenotypes in the cohorts provides trajectories throughout the lifespan. Trajectories were estimated in the full dataset including patients and by excluding diagnostic groups in each cohort separately.

Genome-wide association analysis. At each participating site, genotypes were imputed using the 1000 Genomes project dataset[58] through the Michigan Imputation Server[59] (https://imputationserver.sph.umich.edu/) or the Sanger Imputation Server[60] (Supplementary Table 3). Subsequently, each site ran the same multi-dimensional scaling (MDS) analysis protocol, computing MDS components from the combination of their cohort's data with the HapMap3 population[61]. This ensured that all sites corrected for ancestry in a consistent manner. See http://enigma.ini.usc.edu/protocols/genetics-protocols/ for the imputation and MDS analysis protocol. Within each cohort, genome-wide association was conducted using an additive model, modeling change rate as a function of the genetic variant plus covariates age, sex, age × sex, age^2, age^2 × sex and ancestry (the first four MDS components). Although it is possible that rates of brain structural changes are different in males and females, we did not have the power to perform analyses separating the sexes. Dummy variables were added where appropriate—for example, when multiple scanners were used. We re-ran these analyses adding a covariate for disease status if the cohorts contained patients and controls. Most sites used our harmonized GWAS protocol, which used raremetalworker[62] for analysis (Supplementary Table 3). Regardless of the study design, a kinship matrix was incorporated in these analyses, accounting for relatedness in family studies or possible unknown kinship in the other studies.

Given the small sample sizes of the individual cohorts, a stringent cohort-level quality control was enforced, to exclude variants with a minor allele frequency < 0.05 or variants with imputation R^2 / info score <0.75. Across cohorts and phenotypes, GWAS summary plots (Manhattan plots and Q–Q plots) were visually inspected at the central site. If a given cohort or trait showed deviation from expectations, sites were asked to re-analyze their data, which usually involved removal of outliers in the phenotypic data. Q–Q plots per cohort, per phenotype can be found in Supplementary Fig. 10.

Meta-analysis and meta-regression. In the phase 1 cohorts of European ancestry ($n = 9,604$), we aggregated the cohort-level data for each phenotype, using standard-error-weighted meta-analysis or meta-regression. We employed a cumulative meta-analysis and meta-regression approach for replication in phase 2 ($n = 15,100$). The meta-regression could not be performed separately in the three independent cohorts added in phase 2 because a regression line based on three points is prone to overfitting. For age-independent analyses, we list results in the added sample (Supplementary Tables 4 and 10). We tested three models. Under the assumption that effect sizes of SNPs were consistent across the lifespan (that is, a standard meta-analytic approach), where the subscript C denotes a cohort and ε an error term:

1. Effect_SNP$_C$ ~ $b_0 + \varepsilon_C$, under the null hypothesis that $b_0 = 0$.
Given that brain changes throughout life are dependent on age, the effects of a genetic variant on brain change are likely to depend on age, too. Within cohorts, such an age by SNP effect analysis would not have been feasible because longitudinal cohorts that span the age range between 4 and 99 years do not exist. Given the widespread mean age among the cohorts included (Extended Data Fig. 1 and Supplementary Table 1), it was possible to calculate the age-dependent effects across the lifespan by comparing effects of loci between cohorts, through meta-regression. Meta-regression is a sophisticated tool for addressing heterogeneity between cohorts in meta-analyses when the source of heterogeneity is known (in this case, age)[63]. We estimated the following model under the assumption that the effects of SNPs may vary in size or direction across the lifespan:
2. Effect_SNP$_C$ ~ $b_0 + b_1 \times \text{age}_C + \varepsilon_C$ under the null hypothesis that $b_1 = 0$ (1 degree of freedom) and
3. Effect_SNP$_C$ ~ $b_0 + b_1 \times \text{age}_C + b_2 \times \text{age}_C{}^2 + \varepsilon_C$ under the null hypothesis that ($b_1 = b_2 = 0$, 2 degrees of freedom).

SNP data were aligned using METAL[64] for all three analyses. The age-independent effect of SNPs (model 1) was computed in METAL. For the age-dependent analyses (model 2 for linear age effects and model 3 for quadratic age effects), the aligned data were imported into R[52], and fixed effects meta-regression was performed using the R package metafor[65] (version 2.0-0). Results were filtered on SNPs that were present for at least 50% of the cohorts and in at least 50% of the individuals.

Functional mapping. Functional mapping was performed using the Functional Mapping and Annotation (FUMA) platform designed for prioritization, annotation and interpretation of GWAS results[66]. As the first step, independent significant SNPs in the individual GWAS meta-analysis summary statistics were identified based on their *P* value ($P < 5 \times 10^{-8}$) and independence of each other ($r^2 < 0.6$ in the 1000 Genomes phase 3 reference) within a 1-Mb window. Thereafter, lead SNPs were identified from independent significant SNPs, which are independent of each other ($r^2 < 0.1$). We used FUMA to annotate lead SNPs in genomic risk loci based on the following functional consequences on genes: eQTL data (GTEx version 6 and version 7 (ref. [67])), blood eQTL browser[68], BIOS QTL browser[69], BRAINEAC[70], MuTHER[71], xQTLServer[72], the CommonMind Consortium[73] and three-dimensional chromatin interactions from Hi-C experiments of 21 tissues and cell types[74]. Next, for eQTL mapping and chromatin interaction mapping, genes were mapped using positional mapping, which is based on a maximum distance between SNPs (default 10 kb) and genes. Chromatin interaction mapping was performed with significant chromatin interactions (defined as FDR < 1×10^{-6}). The two ends of significant chromatin interactions were defined as follows: region 1—a region overlapping with one of the candidate SNPs; and region 2—another end of the significant interaction, used to map to genes based on overlap with a promoter region (250 bp upstream and 50 bp downstream of the transcription start site).

Visualization of SNP effects. We visualized the effects of our top SNPs on the lifespan trajectory, assuming no effects of the other SNPs, for easier interpretation of the direction of effect. Similarly to the estimation of the lifespan trajectory, we estimated a smoothed version $f(x)$ of the phenotypic change rate using LOWESS (see above) and integrated the rate of change. We added the unknown volume *C* at the start of our age range by fitting the integrated curve to the baseline data. Suppose $h(x)$ is the unknown rate of change for non-carriers. The additional change rate $g(x)$ for carriers was estimated through the meta-analysis or meta-regression. The full dataset contained a fraction *p* of the carriers of the tested allele. Assuming $p + q = 1$, $f(x) = p \times (h(x) + g(x)) + q \times h(x) = h(x) + p \times g(x)$. We created a rate of change curve for non-carriers as $f(x) - p \times g(x)$ and a rate of change curve of carriers as $f(x) + q \times g(x)$. The offset *C* is potentially different in carriers and non-carriers, so we estimated this difference by taking the effect of the cross-sectional GWAS data (see below) in this SNP or a proxy SNP in high linkage disequilibrium (LD).

Gene-based and gene set analyses. Gene-based associations with 15 phenotypes were estimated using MAGMA[75] (version 1.09a) using the summary statistics from age-independent and age-dependent GWAS meta-analyses of rate of change of global brain measures. Gene names and locations were based on NCBI 37.3 locations as provided by MAGMA. Association was tested using the SNP-wise mean model, in which the sum of −log(SNP *P* value) for SNPs located within the transcribed region was used as the test statistic. LD correction was based on estimates from the 1000 Genomes Project phase 3 European ancestry samples[58]. To describe the direction of the age effect for significant genes in the age-dependent analyses, we subsequently identified the SNPs that were used in the gene-based *P* value and plotted the age-dependent effect of the top SNP that contributed to the gene-based *P* value.

The generated gene-based *P* values were used to analyze sets of genes to test for association of genes belonging to specific biological pathways or processes. MAGMA applies a competitive test to analyze if the genes of a gene set are more strongly associated with the trait than other genes while correcting for a series of confounding effects, such as gene length and size of the gene set. For gene sets, we used 9,975 sets with 10–1,000 genes from the GO sets[76] curated from Molecular Signatures Database 7.0 (ref. [77]).

Multiple testing corrections. We investigated annual rates of change for 15 brain phenotypes, but these are correlated to some extent (Extended Data Fig. 2). We, therefore, estimated the effective number of independent variables based on matrix spectral decomposition[78] for the largest adolescent cohort (IMAGEN; $n=1{,}068$) and for the largest elderly cohort from the phase 1 sample (ADNI2; $n=626$). The most conservative estimate of the number of independent traits was 13.93. Despite the fact that models 2 and 3 are nested and, therefore, not independent, we also corrected for performing three analyses per trait. The study-wide significant threshold for the genome was, therefore, set at $P<1.2\times10^{-9}$ ($5\times10^{-8}/13.93\times3$). For gene-based significance, we applied a genome-wide significance level of $0.05/17{,}541=2.85\times10^{-6}$ and a study-wide significance of $2.85\times10^{-6}/(13.93\times3)$—that is, $P<6.82\times10^{-8}$. For gene set significance, we applied a genome-wide significance level of $0.05/9{,}975=5.01\times10^{-6}$ and a study-wide significance level of $5.01\times10^{-6}/(13.93\times3)$—that is, $P<1.20\times10^{-7}$.

SNP heritability. SNP heritabilities, h^2_{SNP}, were estimated by using linkage disequilibrium score regression[79] (LDSR) for the European ancestry brain change GWAS to ensure matching of population LD structure. For LDSR, we used pre-computed LD scores based on the European ancestry samples of the 1000 Genomes Project[58] restricted to HapMap3 SNPs[61]. The summary statistics with standard LDSC filtering were regressed onto these scores. SNP heritabilities were estimated based on the slope of the LDSR, with heritabilities on the observed scale calculated. To ensure sufficient power for the genetic correlations, r_g was calculated if the z-score of the h^2_{SNP} for the corresponding GWAS was 4 or higher[79].

Comparison with cross-sectional results. For the genome-wide significant genes and genes associated with genome-wide significant SNPs, we compared our findings with cross-sectional GWAS summary statistics when available. To this end, datasets[26,40–42] were requested and downloaded from http://enigma.ini.usc.edu/research/download-enigma-gwas-results/ and http://big.stats.ox.ac.uk/download_page. Gene-based association analyses for cross-sectional brain GWAS summary statistics were performed using MAGMA (as described above). Additionally, we compared the overlap in the first 1,000 ranked genes to the expected number of overlapping genes based on chance. FDR correction[80] was applied to determine over-representation or under-representation of genes from our longitudinal GWAS to the cross-sectional previously published GWAS[26,40–42].

Overlap with cross-sectional results and other traits. To investigate genetic overlap with other traits across the genome, we applied an adapted version of iSECA[81] that examines pleiotropy and concordance of the direction of effects between two phenotypes by comparing expected and observed overlap in sets of SNPs from both phenotypes that are thresholded at different levels. From the results at each threshold, heat map plots were generated containing binomial tests for pleiotropy and Fisher's exact tests for concordance. An empirical *P* value for overall pleiotropy and concordance was then generated through permutation testing. Our implementation of iSECA also included a *P* value for overall discordance, as we expect some phenotypes to negatively influence brain structural change rates. *P* values were computed using a two-step approach. We first ran 1,000 permutations. If the *P* value for pleiotropy was below 0.05/15, we re-ran the analyses with 10,000 permutations to obtain a more precise *P* value. Summary statistics of change rates were first filtered on SNPs for which more than 95% of the individuals contributed data to remove the sample size dependency of *P* values and subsequently clumped ($P=1$, $kb=1{,}000$) to ensure independence of input SNPs.

We investigated the genetic overlap between brain structural changes and risk for 20 neuropsychiatric, neurological and somatic disorders and physical and psychological traits. Summary statistics were downloaded or requested for aggression[82], alcohol dependence[83], AD[84], attention-deficit/hyperactivity disorder[85], autism[86], bipolar disorder[87], BMI[30], brain age gap[12], cognitive functioning[29], depression[27], type 2 diabetes[88], ever-smoking[32], focal epilepsy[89], height[30], inflammatory bowel disease[90], insomnia[31], multiple sclerosis[91], Parkinson's disease[92], rheumatoid arthritis[93] and schizophrenia[28]. These phenotypes were chosen because of known associations with brain structure or function and availability of summary statistics based on large GWASs. For comparison, we computed the genetic overlap between cross-sectional brain structure and these phenotypes, using the same method.

Apart from these, we also (1) included intracranial volume[94] to investigate the effect of overall head size and (2) tested the overlap between each structure's longitudinal change measure against its cross-sectional brain structure. Pleiotropy, concordance or discordance was considered significant when the *P* value was smaller than $0.05/15\times22$ (number of change rates × number of phenotypes tested) $=1.5\times10^{-4}$.

Brain gene expression. GENE2FUNC, a core process of FUMA[66], was employed to analyze gene expression patterns. For this, a set of eight genes was used as input, including all genome-wide significant genes and genes harboring genome-wide significant SNPs (compare Supplementary Tables 5, 7, 9 and 11). A gene expression heat map was constructed employing GTEx version 8 (ref. [33]) (54 tissue types) and BrainSpan RNA sequencing data across 29 different ages or 11 different developmental stages[32]. The average of normalized expression per label (zero means across samples) was displayed on the corresponding heat maps. Expression values are transcripts per million (TPM) for GTEx version 8 and reads per kilobase of transcript, per million mapped reads (RPKM) in the case of the BrainSpan dataset.

Phenome-wide association studies. To identify phenotypes associated with the candidate SNPs and genes (defined as genome-wide significant SNPs and the genome-wide significant genes and genes associated with genome-wide significant SNPs), a pheWAS was done for each SNP and/or gene. pheWAS was performed using public data provided by GWAS Atlas[32] (https://atlas.ctglab.nl). To correct for multiple testing, the total number of GWASs (4,756) was considered (including GWASs in which the searched SNP or gene was not tested) and the number of tested SNPs and genes ($n=14$), resulting in a Bonferroni-corrected *P* value threshold of $1.05\times10^{-5}/14$—that is, $P<7.51\times10^{-7}$.

Sensitivity analyses. The phase 2 analyses include available data from all cohorts with European ancestry ($n=15{,}100$). The four cohorts of non-European and mixed ancestry together consist of 540 individuals who are predominantly children and adolescents (Supplementary Table 3). The number of individuals, heterogeneity in ancestry and the age distribution do not allow for separate meta-analysis or meta-regression. We, therefore, added the cohorts of non-European ancestry to the original datasets and re-ran analyses ($n=15{,}640$). In a second analysis, we excluded the nine cohorts that had $n<75$ or mean scanning interval <0.5 years (Supplementary Table 2), leaving $n=14{,}601$ individuals. The main analyses include data from all individuals combined, without correction for disease. This approach was chosen because many neurological and neuropsychiatric diseases are characterized by aberrant brain changes over time, and genes involved in the disease may also be involved in these brain changes. To check whether our results were confounded by disease, we repeated the main analyses excluding diagnostic groups of each cohort ($n=13{,}390$) and by correcting for disease status.

Reporting Summary. Further information on research design is available in the Nature Research Reporting Summary linked to this article.

Data availability

This work is a meta-analysis. Upon publication, the meta-analytic results will be made available from the ENIGMA consortium webpage (http://enigma.ini.usc.edu/research/download-enigma-gwas-results). Cohort-level data can be shared upon reasonable request, after permission of cohort principal investigators. Individual-level data can be shared with interested investigators, subject to local and national ethics regulations and legal requirements that respect the informed consent forms and national laws of the country of origin of the persons scanned. Figures that contain cohort-level (meta) data are as follows: Figs. 1 and 2, Extended Data Figs. 1, and 2 and Supplementary Figs 1, 3, 8 and 10.
Public data used in this work include the ABCD cohort (data release 3.0, accessible through https://nda.nih.gov/abcd; https://doi.org/10.15154/1519007), the ADNI cohort (accessible through adni.loni.usc.edu) and the UK Biobank cohort (data request 11559, https://www.ukbiobank.ac.uk).

Code availability

The code for processing of individual cohorts (including imaging and quality control, imputation and GWAS protocol) can be found on http://enigma.ini.usc.edu/ongoing/enigma-plasticity-working-group/. Code for the meta-regression is available through GitHub (https://github.com/RMBrouwer/GWAS_meta_regression).

References

49. Fischl, B. et al. Whole brain segmentation: automated labeling of neuroanatomical structures in the human brain. *Neuron* **33**, 341–355 (2002).
50. Fischl, B. et al. Sequence-independent segmentation of magnetic resonance images. *Neuroimage* **23**, S69–S84 (2004).
51. Reuter, M., Schmansky, N. J., Rosas, H. D. & Fischl, B. Within-subject template estimation for unbiased longitudinal image analysis. *Neuroimage* **61**, 1402–1418 (2012).
52. Iscan, Z. et al. Test–retest reliability of freesurfer measurements within and between sites: effects of visual approval process. *Hum. Brain Mapp.* **36**, 3472–3485 (2015).

53. Wonderlick, J. S. et al. Reliability of MRI-derived cortical and subcortical morphometric measures: effects of pulse sequence, voxel geometry, and parallel imaging. *Neuroimage* **44**, 1324–1333 (2009).
54. Liem, F. et al. Reliability and statistical power analysis of cortical and subcortical FreeSurfer metrics in a large sample of healthy elderly. *Neuroimage* **108**, 95–109 (2015).
55. Voevodskaya, O. et al. The effects of intracranial volume adjustment approaches on multiple regional MRI volumes in healthy aging and Alzheimer's disease. *Front. Aging Neurosci.* **6**, 264 (2014).
56. Cleveland, W. S. LOWESS: a program for smoothing scatterplots by robust locally weighted regression. *Am. Stat.* **35**, 10–11 (1981).
57. The R Core Team. R: a language and environment for statistical computing. https://www.r-project.org/
58. The 1000 Genomes Consortium. A global reference for human genetic variation. *Nature* **526**, 68–74 (2015).
59. Das, S. et al. Next-generation genotype imputation service and methods. *Nat. Genet.* **48**, 1284–1287 (2016).
60. McCarthy, S. et al. A reference panel of 64,976 haplotypes for genotype imputation. *Nat. Genet.* **48**, 1279–1283 (2016).
61. International HapMap Consortium. Integrating common and rare genetic variation in diverse human populations. *Nature* **467**, 52–58 (2010).
62. Feng, S., Liu, D., Zhan, X., Wing, M. K. & Abecasis, G. R. RAREMETAL: fast and powerful meta-analysis for rare variants. *Bioinformatics* **30**, 2828–2829 (2014).
63. Baker, W. L., Michael White, C., Cappelleri, J. C., Kluger, J. & Coleman, C. I. Understanding heterogeneity in meta-analysis: the role of meta-regression. *Int. J. Clin. Pract.* **63**, 1426–1434 (2009).
64. Willer, C. J., Li, Y. & Abecasis, G. R. METAL: fast and efficient meta-analysis of genome-wide association scans. *Bioinformatics* **26**, 2190–2191 (2010).
65. Viechtbauer, W. Conducting meta-analyses in R with the metafor package. *J. Stat. Softw.* **36**, 1–48 (2010).
66. Watanabe, K., Taskesen, E., Van Bochoven, A. & Posthuma, D. Functional mapping and annotation of genetic associations with FUMA. *Nat. Commun.* **8**, 1826 (2017).
67. Lonsdale, J. et al. The Genotype-Tissue Expression (GTEx) project. *Nat. Genet.* **45**, 580–585 (2013).
68. Westra, H. J. et al. Systematic identification of *trans* eQTLs as putative drivers of known disease associations. *Nat. Genet.* **45**, 1238–1243 (2013).
69. Zhernakova, D. V. et al. Identification of context-dependent expression quantitative trait loci in whole blood. *Nat. Genet.* **49**, 139–145 (2017).
70. Ramasamy, A. et al. Genetic variability in the regulation of gene expression in ten regions of the human brain. *Nat. Neurosci.* **17**, 1418–1428 (2014).
71. Grundberg, E. et al. Mapping *cis*-and *trans*-regulatory effects across multiple tissues in twins. *Nat. Genet.* **44**, 1084–1089 (2012).
72. Ng, B. et al. An xQTL map integrates the genetic architecture of the human brain's transcriptome and epigenome. *Nat. Neurosci.* **20**, 1418–1426 (2017).
73. Fromer, M. et al. Gene expression elucidates functional impact of polygenic risk for schizophrenia. *Nat. Neurosci.* **19**, 1442–1453 (2016).
74. Schmitt, A. D. et al. A compendium of chromatin contact maps reveals spatially active regions in the human genome. *Cell Rep.* **17**, 2042–2059 (2016).
75. de Leeuw, C. A., Mooij, J. M., Heskes, T. & Posthuma, D. MAGMA: generalized gene-set analysis of GWAS data. *PLoS Comput. Biol.* **11**, e1004219 (2015).
76. The Gene Ontology Consortium. Gene Ontology Consortium: going forward. *Nucleic Acids Res.* **43**, D1049–D1056 (2015).
77. Subramanian, A. et al. Gene set enrichment analysis: a knowledge-based approach for interpreting genome-wide expression profiles. *Proc. Natl Acad. Sci. USA* **102**, 15545–15550 (2005).
78. Nyholt, D. R. A simple correction for multiple testing for single-nucleotide polymorphisms in linkage disequilibrium with each other. *Am. J. Hum. Genet.* **74**, 765–769 (2004).
79. Bulik-Sullivan, B. K. et al. LD score regression distinguishes confounding from polygenicity in genome-wide association studies. *Nat. Genet.* **47**, 291–295 (2015).
80. Benjamini, Y. & Hochberg, Y. Controlling the false discovery rate: a practical and powerful approach to multiple testing. *J. R. Stat. Soc.* **57**, 289–300 (1995).
81. Nyholt, D. R. SECA: SNP effect concordance analysis using genome-wide association summary results. *Bioinformatics* **30**, 2086–2088 (2014).
82. Pappa, I. et al. A genome-wide approach to children's aggressive behavior: the EAGLE consortium. *Am. J. Med. Genet. B Neuropsychiatr. Genet.* **171**, 562–572 (2016).
83. Walters, R. K. et al. Transancestral GWAS of alcohol dependence reveals common genetic underpinnings with psychiatric disorders. *Nat. Neurosci.* **21**, 1656–1669 (2018).
84. Lambert, J. C. et al. Meta-analysis of 74,046 individuals identifies 11 new susceptibility loci for Alzheimer's disease. *Nat. Genet.* **45**, 1452–1458 (2013).
85. Demontis, D. et al. Discovery of the first genome-wide significant risk loci for attention deficit/hyperactivity disorder. *Nat. Genet.* **51**, 63–75 (2019).
86. Psychiatric Genomics Consortium. Meta-analysis of GWAS of over 16,000 individuals with autism spectrum disorder highlights a novel locus at 10q24.32 and a significant overlap with schizophrenia. *Mol. Autism* **8**, 21 (2017).
87. Stahl, E. & Bipolar Working Group of the Psychiatric Genomics Consortium. Genome-wide association study identifies twenty new loci associated with bipolar disorder. *Eur. Neuropsychopharmacol.* **29**, S816 (2019).
88. Scott, R. A. et al. An expanded genome-wide association study of type 2 diabetes in Europeans. *Diabetes* **66**, 2888–2902 (2017).
89. The International League Against Epilepsy Consortium on Complex Epilepsies. Genome-wide mega-analysis identifies 16 loci and highlights diverse biological mechanisms in the common epilepsies. *Nat. Commun.* **9**, 5269 (2018).
90. Liu, J. Z. et al. Association analyses identify 38 susceptibility loci for inflammatory bowel disease and highlight shared genetic risk across populations. *Nat. Genet.* **47**, 979–986 (2015).
91. Sawcer, S. et al. Genetic risk and a primary role for cell-mediated immune mechanisms in multiple sclerosis. *Nature* **476**, 214–219 (2011).
92. Nalls, M. A. et al. Large-scale meta-analysis of genome-wide association data identifies six new risk loci for Parkinson's disease. *Nat. Genet.* **46**, 989–993 (2014).
93. Okada, Y. et al. Genetics of rheumatoid arthritis contributes to biology and drug discovery. *Nature* **506**, 376–381 (2014).
94. Adams, H. H. et al. Novel genetic loci underlying human intracranial volume identified through genome-wide association. *Nat. Neurosci.* **19**, 1569–1582 (2016).

Acknowledgements

Data used in preparing this article were obtained from the Alzheimer's Disease Neuroimaging Initiative (ADNI) database (adni.loni.usc.edu). As such, many investigators within the ADNI contributed to the design and implementation of ADNI and/or provided data but did not participate in analysis or writing of this report. A complete listing of ADNI investigators may be found at http://adni.loni.usc.edu/wp-content/uploads/how_to_apply/ADNI_Acknowledgement_List.pdf. A full list of consortium authors can be found in the Supplementary Information. Funding: The ENIGMA-Plasticity Working Group is part of the ENIGMA World Aging Center, funded by NIA grants R56 AG058854 and R01 AG058854. The ENIGMA Consortium core funding was supported by NIH Consortium Grant U54 EB020403, supported by a cross-NIH alliance that funds Big Data to Knowledge Centers of Excellence. 1000BRAINS: 1000BRAINS is a population-based cohort based on the Heinz-Nixdorf Recall Study and is supported, in part, by the German National Cohort. We thank the Heinz Nixdorf Foundation (Germany) for their generous support in terms of the Heinz Nixdorf Study. The authors are supported by the Initiative and Networking Fund of the Helmholtz Association (Svenja Caspers) and the European Union's Horizon 2020 Research and Innovation Programme under grant agreements 785907 (Human Brain Project SGA2; Svenja Caspers, Sven Cichon and Katrin Amunts). This work was further supported by the German Federal Ministry of Education and Research (BMBF) through the Integrated Network IntegraMent (Integrated Understanding of Causes and Mechanisms in Mental Disorders) under the auspices of the e:Med Program (grant 01ZX1314A; Sven Cichon) and by the Swiss National Science Foundation (SNSF, grant 156791; Sven Cichon). ABCD: Data used in the preparation of this article were obtained from the Adolescent Brain Cognitive Development (ABCD) Study (https://abcdstudy.org), held in the NIMH Data Archive (NDA). This is a multi-site, longitudinal study designed to recruit more than 10,000 children aged 9–10 years and follow them over 10 years into early adulthood. The ABCD Study is supported by the National Institutes of Health and additional federal partners under award numbers U01DA041048, U01DA050989, U01DA051016, U01DA041022, U01DA051018, U01DA051037, U01DA050987, U01DA041174, U01DA041106, U01DA041117, U01DA041028, U01DA041134, U01DA050988, U01DA051039, U01DA041156, U01DA041025, U01DA041120, U01DA051038, U01DA041148, U01DA041093, U01DA041089, U24DA041123 and U24DA041147. A full list of supporters is available at https://abcdstudy.org/federal-partners.html. A listing of participating sites and a complete listing of the study investigators can be found at https://abcdstudy.org/consortium_members/. ABCD consortium investigators designed and implemented the study and/or provided data but did not necessarily participate in the analysis or writing of this report. This manuscript reflects the views of the authors and may not reflect the opinions or views of the NIH or ABCD consortium investigators. The ABCD data repository grows and changes over time. The ABCD data used in this report came from Data Release 3.0 (https://doi.org/10.15154/1519007). ADNI: Data collection and sharing for this project was funded by the Alzheimer's Disease Neuroimaging Initiative (ADNI) (National Institutes of Health Grant U01 AG024904) and DOD ADNI (Department of Defense award number W81XWH-12-2-0012). ADNI is funded by the National Institute on Aging, the National Institute of Biomedical Imaging and Bioengineering and through generous contributions from the following: AbbVie, Alzheimer's Association; Alzheimer's Drug Discovery Foundation; Araclon Biotech; BioClinica, Inc.; Biogen; Bristol Myers Squibb; CereSpir, Inc.; Cogstate; Eisai Inc.; Elan Pharmaceuticals, Inc.; Eli Lilly and Company; EuroImmun; F. Hoffmann-La Roche Ltd and its affiliated company Genentech, Inc.; Fujirebio; GE Healthcare; IXICO Ltd.; Janssen Alzheimer Immunotherapy Research & Development, LLC.; Johnson & Johnson Pharmaceutical

Research & Development LLC.; Lumosity; Lundbeck; Merck & Co., Inc.; Meso Scale Diagnostics, LLC.; NeuroRx Research; Neurotrack Technologies; Novartis Pharmaceuticals Corporation; Pfizer Inc.; Piramal Imaging; Servier; Takeda Pharmaceutical Company; and Transition Therapeutics. The Canadian Institutes of Health Research is providing funds to support ADNI clinical sites in Canada. Private sector contributions are facilitated by the Foundation for the National Institutes of Health (www.fnih.org). The grantee organization is the Northern California Institute for Research and Education, and the study is coordinated by the Alzheimer's Therapeutic Research Institute at the University of Southern California. ADNI data are disseminated by the Laboratory for Neuro Imaging at the University of Southern California. ALS Utrecht: The authors acknowledge grants supporting their work from the European Union's Horizon 2020 Research and Innovation Programme (H2020/2014–2020) under grant agreements 667302 (CoCA), 728018 (Eat2beNICE), 785907 (HBP SGA2) and 772376 (EScORIAL) and the Netherlands ALS Foundation. BDC: Brain Dynamics Centre (BDC), Sydney—cohort is funded by a National Health & Medical Research Council of Australia Project Grant (APP1008080). BHRCS: The Brazilian High Risk Cohort Study (BHRCS) was supported by the National Institute of Developmental Psychiatry for Children and Adolescents (INPD) Grant: Fapesp 2014/50917-0 CNPq 465550/2014-2. BIG: This study used the BIG database, which was established in Nijmegen in 2007. This resource is now part of Cognomics, a joint initiative by researchers of the Donders Centre for Cognitive Neuroimaging, the Human Genetics and Cognitive Neuroscience departments of the Radboud University Medical Center and the Max Planck Institute for Psycholinguistics. The Cognomics Initiative is supported by the participating departments and centers and by external grants, including grants from the Biobanking and Biomolecular Resources Research Infrastructure (Netherlands) (BBMRI-NL) and the Hersenstichting Nederland. In particular, the authors would also like to acknowledge grants supporting their work from the Netherlands Organization for Scientific Research (NWO)—that is, the NWO Brain & Cognition Excellence Program (grant 433-09-229) and the Vici Innovation Program (grant 016-130-669 to B.F.). Additional support is received from the European Community's Seventh Framework Programme (FP7/2007—2013) under grant agreements n° 602805 (Aggressotype), n° 603016 (MATRICS), n° 602450 (IMAGEMEND) and n° 278948 (TACTICS) and from the European Community's Horizon 2020 Programme (H2020/2014—2020) under grant agreements n° 643051 (MiND) and n° 667302 (CoCA). BrainSCALE: The BrainSCALE study is a collaborative project between Netherlands Twin Register (NTR) at the Vrije Universiteit (VU) Amsterdam and University Medical Center Utrecht (UMCU). The BrainSCALE study was funded by Nederlandse Organisatie voor Wetenschappelijk Onderzoek (NWO 51.02.061 to H.E.H., NWO 51.02.062 to D.B., NWO-NIHC Programs of Excellence 433-09-220 to H.E.H., NWO-MagW 480-04-004 to D.B. and NWO/SPI 56-464-14192 to D.B.); FP7 Ideas: the European Research Council (ERC-230374 to D.B.), Universiteit Utrecht (High Potential Grant to H.E.H.), Netherlands Twin Registry Repository (NWO-Groot 480-15-001/674 to D.B.) and Neuroscience Campus Amsterdam (NCA). Biomolecular Resources Research Infrastructure (BBMRI–NL, 184.021.007 and 184.033.111) developmental trajectories of psychopathology (NIMH 1RC2 MH089995); and the Avera Institute for Human Genetics. Cape Town: The CTAAC study was supported by grant R01-HD074051. DBSOS: The DBSOS study is partially funded by the Brain and Behavior Foundation (NARSAD) by an Independent Investigator grant (20244). The Generation R Study is made possible by financial support from the Erasmus Medical Center, Rotterdam, and the Netherlands Organization for Health Research and Development (ZonMW). The neuroimaging infrastructure is supported by ZonMW TOP (912110210), the NWO Physical Sciences Division and the SURFsara supercomputing center (Cartesius Compute Cluster). FOR2107: This work is part of the German multicenter consortium 'Neurobiology of affective disorders. A translational perspective on brain structure and function', funded by the German Research Foundation (Deutsche Forschungsgemeinschaft (DFG); Forschungsgruppe/Research Unit FOR2107). Grant agreements included the following: FOR2107 DA1151/5-1 and DA1151/5-2 to U.D.; SFB-TRR58, Projects C09 and Z02 to U.D.; the Interdisciplinary Center for Clinical Research (IZKF) of the Medical Faculty of Münster (grant Dan3/012/17 to U.D.); KR 3822/7-1 and KR 3822/7-2 to A.K.; KI 588/14-1 and KI 588/14-2; and NO 246/10-1 and NO 246/10-2 to M.M.N. A.J. was in particular involved as principal investigator in WP6, multi-method data analytics (JA 1890/7-1 and JA 1890/7-2). The FOR2107 study was also supported by the German Federal Ministry of Education and Research (BMBF), through ERA-NET NEURON, 'SynSchiz: linking synaptic dysfunction to disease mechanisms in schizophrenia—a multilevel investigation' (01EW1810 to M.R.) and the German Research Foundation (DFG grant FOR2107; RI908/11-2 to M.R.). Generation R: Netherlands Organization for Health Research and Development (ZonMw) TOP project 91211021. Sophia Children's Hospital Foundation (Stichting Vrienden van het Sophia) project S18-68. The Generation R sample further reports the following support: Supercomputing resources for imaging processing were supported by the NWO Physical Sciences Division (Exacte Wetenschappen) and SURFsara (Cartesius compute cluster, https://www.surf.nl); neuroimaging data analysis was supported, in part, by Sophia Foundation Project S18-20 and Erasmus University Fellowship awarded to R.L.M. HGUGM: This work was supported by Spanish Ministry of Science and Innovation, Instituto de Salud Carlos III (SAM16PE07CP1, PI16/02012 and PI19/024), co-financed by ERDF Funds from the European Commission, 'A way of making Europe', CIBERSAM; Madrid Regional Government (B2017/BMD-3740 AGES-CM-2), European Union Structural Funds; European Union Seventh Framework Program under grant agreements FP7- HEALTH-2013-2.2.1-2-603196 (Project PSYSCAN) and European Union H2020 Program under the Innovative Medicines Initiative 2 Joint Undertaking (grant agreement 115916, Project PRISM and grant agreement 777394, Project AIMS-2-TRIALS), Fundación Familia Alonso, Fundación Alicia Koplowitz and Fundación Mutua Madrileña. HUBIN: The HUBIN study was funded by the Swedish Research Council (2003-5485, 2006-2992, 2006-986, 2008-2167, K2012-61X-15078-09-3, 521-2011-4622, 521-2014-3487 and 2017-00949); regional agreement on medical training and clinical research between the Stockholm County Council and the Karolinska Institutet; and the Knut and Alice Wallenberg Foundation. IMAGEN: This work received support from the following sources: the European Union-funded FP6 Integrated Project IMAGEN (Reinforcement-related behaviour in normal brain function and psychopathology) (LSHM-CT- 2007-037286), the Horizon 2020 funded ERC Advanced Grant 'STRATIFY' (Brain network based stratification of reinforcement-related disorders) (695313), ERANID (Understanding the interplay between cultural, biological and subjective factors in drug use pathways) (PR-ST-0416-10004), BRIDGET (JPND: BRain Imaging, cognition dementia and next generation GEnomics) (MR/N027558/1), Human Brain Project (HBP SGA 2, 785907), the FP7 project MATRICS (603016), the Medical Research Council Grant 'c-VEDA' (Consortium on Vulnerability to Externalizing Disorders and Addictions) (MR/N000390/1), the National Institute for Health Research (NIHR) Biomedical Research Centre at South London and Maudsley NHS Foundation Trust and King's College London, the Bundesministerium für Bildung und Forschung (BMBF grants 01GS08152 and 01EV0711 and Forschungsnetz AERIAL 01EE1406A and 01EE1406B), Deutsche Forschungsgemeinschaft (DFG grants SM 80/7-2, SFB 940, TRR 265 and NE 1383/14-1), the Medical Research Foundation and Medical Research Council (grants MR/R00465X/1 and MR/S020306/1) and the National Institutes of Health (NIH)-funded ENIGMA (grants 5U54EB020403-05 and 1R56AG058854-01). Further support was provided by grants from the ANR (ANR-12-SAMA-0004, AAPG2019–GeBra), the Eranet Neuron (AF12-NEUR0008-01–WM2NA and ANR-18-NEUR00002-01–ADORe), the Fondation de France (00081242), the Fondation pour la Recherche Médicale (DPA20140629802), the Mission Interministérielle de Lutte-contre-les-Drogues-et-les-Conduites-Addictives (MILDECA), the Assistance-Publique-Hôpitaux-de-Paris and INSERM (interface grant), Paris Sud University IDEX 2012, the Fondation de l'Avenir (grant AP-RM-17-013), the Fédération pour la Recherche sur le Cerveau; the National Institutes of Health, Science Foundation Ireland (16/ERCD/3797), U.S.A. (Axon, Testosterone and Mental Health during Adolescence; RO1 MH085772-01A1) and by NIH Consortium grant U54 EB020403, supported by a cross-NIH alliance that funds Big Data to Knowledge Centres of Excellence. LBC1936: We thank the Lothian Birth Cohort 1936 members who took part in this study and Lothian Birth Cohort 1936 research team members and radiographers who collected, entered and checked data used in this paper. MRI acquisition and analyses were conducted at the Brain Research Imaging Centre, Neuroimaging Sciences, University of Edinburgh (www.bric.ed.ac.uk), which is part of the SINAPSE (Scottish Imaging Network—A Platform for Scientific Excellence) collaboration (www.sinapse.ac.uk), funded by the Scottish Funding Council and the Chief Scientist Office. The LBC1936 and this research are supported by Age UK (Disconnected Mind project), the UK Medical Research Council (MRC; G0701120, G1001245, MR/M013111/1 and MR/R024065/1) and the University of Edinburgh. NCNG: The NCNG sample collection was supported by grants from the Bergen Research Foundation and the University of Bergen, the Dr. Einar Martens Fund, the K.G. Jebsen Foundation and the Research Council of Norway, to S.L.H., V.M.S. and T.E. NESDA: The infrastructure for the NESDA study (www.nesda.nl) is funded through the Geestkracht program of the Netherlands Organisation for Health Research and Development (ZonMw, grant 10-000-1002) and financial contributions by participating universities and mental healthcare organizations (VU University Medical Center, GGZ inGeest, Leiden University Medical Center, Leiden University, GGZ Rivierduinen, University Medical Center Groningen, University of Groningen, Lentis, GGZ Friesland, GGZ Drenthe and Rob Giel Onderzoekscentrum). NeuroIMAGE: The NeuroIMAGE study was supported by NIH grant R01MH62873 (to S.V.F.), NWO Large Investment Grant 1750102007010 (to J.B.), ZonMW grant 60-60600-97-193, NWO grants 056-13-015 and 433-09-242 and matching grants from Radboud University Nijmegen Medical Center, University Medical Center Groningen and Accare and Vrije Universiteit Amsterdam. The research leading to these results also received support from the European Community's Seventh Framework Programme (FP7/2007-2013) under grant agreement 278948 (TACTICS), 602805 (Aggressotype), 603016 (MATRICS) and 602450 (Imagemend) and the Innovation Medicine Initiative grants 115300 (EU-AIMS) and 777394 (AIMS-2-TRIALS). NUIG: We would like to thank the radiologists at the University Hospital Galway and the participants who generously gave their time to make this study possible. The NUIG sample was supported and funded by the National University of Ireland Galway (NUIG) Millennium Fund and the Health Research Board (HRA_POR/2011/100). OATS: We gratefully acknowledge and thank the OATS participants, their supporters and the research team. The Older Australian Twin Study (OATS) is supported by Australian NHMRC/Australian Research Council Strategic Award (grant 401162) and NHMRC project grant 1405325. This study was facilitated through Twins Research Australia, a national resource in part supported by a Centre for Research Excellence from the NHMRC. DNA was extracted by Genetic Repositories Australia (NHMRC grant 401184). Genome-wide genotyping at the Diamantina Institute, University of Queensland, was partly funded by a CSIRO Flagship Collaboration Fund Grant. PAFIP: PAFIP was supported by the Instituto de Salud Carlos III (PI14/00639, PI14/00918 and PI17/01056) and Fundación Instituto de Investigación Marqués de Valdecilla (NCT0235832 and NCT02534363). No pharmaceutical company has financially supported the study. Rotterdam Study: The GWAS datasets are supported by the Netherlands Organization of Scientific Research NWO Investments (175.010.2005.011 and 911-03-012), the Genetic Laboratory of the Department of Internal Medicine, Erasmus Medical Center, the Research Institute for Diseases in the Elderly (014-93-015; RIDE2), the Netherlands Genomics Initiative (NGI)/Netherlands Organization for Scientific Research (NWO) and the Netherlands Consortium for Healthy Aging (NCHA), project 050-060-810. We thank P. Arp, M. Jhamai, M. Verkerk, L. Herrera, M. Peters and C. Medina-Gomez for their help in creating the GWAS database and K. Estrada, Y. Aulchenko and C. Medina-Gomez for the creation and analysis of imputed data. The Rotterdam Study is funded by Erasmus Medical Center and Erasmus University, Rotterdam, the Netherlands Organization for the Health Research and Development (ZonMw), the Research Institute for Diseases in the Elderly (RIDE), the Ministry of Education, Culture and Science, the Ministry for Health, Welfare and Sports, the European Commission (DG XII) and the Municipality of Rotterdam. The authors are grateful to the study participants, the staff from the Rotterdam Study and the participating general practitioners and pharmacists. SHIP: The SHIP study is part of the Community Medicine Research net of the University of Greifswald, Germany, which is funded by the Federal Ministry of Education and Research (grants 01ZZ9603, 01ZZ0103 and 01ZZ0403), the Ministry of Cultural Affairs and the Social Ministry of the Federal State of Mecklenburg-West Pomerania. MRI scans in SHIP and SHIP-TREND have been supported by a joint grant from Siemens Healthineers and the Federal State of Mecklenburg-West Pomerania. Sydney MAS: We gratefully acknowledge and thank the Sydney MAS participants, their supporters and the research team. The Sydney Memory and Ageing Study (MAS) is supported by National Health & Medical Research Council of Australia program grants (350833, 568969 and 109308) and a Capacity Building Grant (568940). DNA samples were extracted by Genetic Repositories Australia, an Enabling Facility, which is supported by National Health & Medical Research Council of Australia grant 401184. UK Biobank: This research has been conducted using the UK Biobank Resource under application 11559. UMCU: The UMCU cohort contains a.o. UTWINS and GROUP. UTWINS was funded by the Netherlands Organization for Health Research and Development (ZonMw) (908.02.123 and 917.46.370 to H.E.H.) and by the European Union Marie Curie Research Training Network (MRTN-CT-2006-035987). The GROUP study is partially funded through the Geestkracht programme of the Dutch Health Research Council (Zon-Mw, grant 10-000-1001) and matching funds from participating pharmaceutical companies (Lundbeck, AstraZeneca, Eli Lilly and Janssen Cilag) and universities and mental healthcare organizations (Amsterdam: Academic Psychiatric Centre of the Academic Medical Center and the mental health institutions GGZ Ingeest, Arkin, Dijk en Duin, GGZ Rivierduinen, Erasmus Medical Center and GGZ Noord Holland Noord. Groningen: University Medical Center Groningen and the mental health institutions Lentis, GGZ Friesland, GGZ Drenthe, Dimence, Mediant, GGNet Warnsveld, Yulius Dordrecht and Parnassia psycho-medical center The Hague. Maastricht: Maastricht University Medical Center and the mental health institutions GGzE, GGZ Breburg, GGZ Oost-Brabant, Vincent van Gogh voor Geestelijke Gezondheid, Mondriaan, Virenze riagg, Zuyderland GGZ, MET ggz, Universitair Centrum Sint-Jozef Kortenberg, CAPRI University of Antwerp, PC Ziekeren Sint-Truiden, PZ Sancta Maria Sint-Truiden, GGZ Overpelt and OPZ Rekem. Utrecht: University Medical Center Utrecht and the mental health institutions Altrecht, GGZ Centraal and Delta). UNSW: The UNSW study was supported by the Australian National Medical and Health Research Council (NHMRC) Program Grant 1037196, Project Grant 1066177 and the Lansdowne Foundation. We gratefully acknowledge the Janette Mary O'Neil Research Fellowship to J.M.F. Personal funding: A.L.W.B. received funding from the National Children's Foundation Tallaght, Ireland. R.M.B. was supported by NIA R56AG058854 and R01AG058854 to the ENIGMA World Aging Center. C.D.-C. was supported by Instituto de Salud Carlos III, Juan Rodés Grant (JR19/00024). C.E.F. was supported by R01 AG050595, R01 AG022381, P01 AG055367 and R01R56 AG037985. D.A.l. was supported by the South-Eastern Norway Regional Health Authority (2019107). D.J.S. is supported by the SAMRC. D.v.d.M. was supported by Research Council of Norway grant 276082. E.G.J. was supported by the Swedish Research Council (2003-5485, 2006-2992, 2006-986, 2008-2167, K2012-61X-15078-09-3, 521-2011-4622, 521-2014-3487 and 2017-00949); regional agreement on medical training and clinical research between Stockholm County Council and the Karolinska Institutet; the Knut and Alice Wallenberg Foundation; and the HUBIN project. E.S.P. is supported by Hypatia Tenure Track Grant (Radboudumc); NARSAD Young Investigator Grant (Brain and Behavior Research Foundation ID: 25034); and the Christine Mohrmann Fellowship. E.V. was supported by National Institute for Health Research (NIHR) Biomedical Research Centre at South London and Maudsley NHS Foundation Trust and King's College London. F.N. was supported by German Research Foundation NE 1383/14-1. H.B. was supported by NHMRC Australia. G.A.S. was supported by Conselho Nacional de Desenvolvimento Científico e Tecnológico (CNPq, Brazil; grant 573974/2008-0), the Coordenação de Aperfeiçoamento de Pessoal de Nível Superior (CAPES, Brazil), the Fundação de Amparo à Pesquisa do Estado de São Paulo (FAPESP, Brazil; grant 2008/57896-8) and the Fundação de Amparo à Pesquisa do Estado do Rio Grande do Sul (FAPERGS, Brazil). H.E.H. was supported by NIA R56AG058854 and R01AG058854 to the ENIGMA World Aging Center. H.J.G. has received research funding from the EU Joint Programme Neurodegenerative Disorders (JPND). H.H.H.A. was supported by the Netherlands Organization for Health Research and Development (ZonMW, grant 916.19.151). I.A.B. was supported by University of Sydney Post-graduate Award. I.N. was supported by DFG Ne2254/1-2. J.B.J.K. was supported by NHMRC Dementia Research Team Grant APP1095127. J.H. was supported by R21MH107327-01. J.L.S. was supported by grants R01MH118349 and R01MH120125. J.W. was supported by the UK Dementia Research Institute, which receives its funding from DRI Ltd, funded by the UK Medical Research Council, the Alzheimer's Society and Alzheimer's Research UK (J.W.), the Row Fogo Charitable Trust through the Row Fogo Centre for Research into Ageing and the Brain (AD.ROW4.35 and BRO-D.FID3668413) and the Fondation Leducq Transatlantic Network of Excellence for the Study of Perivascular Spaces in Small Vessel Disease (16 CVD 05). K.L.G. was supported by grant APP1173025. K.S. was supported by research grants from the National Healthcare Group, Singapore (SIG/05004, SIG/05028 and SIG /1103) and the Singapore Bioimaging Consortium (RP C009/2006). L.D. was supported by R01AG059874 and R01MH117601. J.H.F. was supported by SFB 940/2 and the German Ministry of Education and Research (BMBF grants 01EV0711 and 01EE1406B). L.H.v.d.B. was supported by the Netherlands ALS Foundation. O.A.A. was supported by the Research Council of Norway (223273), KG Jebsen Stiftelsen and H2020 CoMorMent (847776). L.M.O.L. was supported by K99MH116115. L.P. received funding from the German Research Foundation (DFG), the Ministry of Science and Education (BMBF) and European Union. L.T.W. is funded by the European Research Council under the European Union's Horizon 2020 Research and Innovation Programme (ERC Starting Grant 802998), the Research Council of Norway (249795), the South-East Norway Regional Health Authority (2019101) and the Department of Psychology, University of Oslo. M.K. was supported by funding from the Dutch National Science Agenda NeurolabNL project (grant 400-17-602). M.L.P.M. was supported by the French funding agency ANR (ANR-12-SAMA-0004), the Assistance-Publique-Hôpitaux-de-Paris and INSERM (interface grant), Paris-Descartes-University (collaborative-project-2010) and Paris-Sud-University (IDEX-2012). M.L.S. was supported by FAPESP: 2016/13737-0 and 2016/04983-7. M.M.N. was supported by the German Research Foundation (DFG grants FOR2107 and NO246/10-2). M.N.S. was supported by the Deutsche Forschungsgemeinschaft (DFG grants TRR 265, SFB 940 and SM 80/7-2) and the German Ministry of Education and Research (BMBF grants 01EV0711 and 01EE1406B). M.R. was supported by DFG FOR2107 RI 908/11-1 and RI 908/11-2 and BMBF Neuron Eranet Synschiz 01EW1810. M.S.K. was supported by the National Health and Medical Research Council, Australia Project Grant (GNT1008080) and Career Development Fellowship (GNT1090148). M.S.P. was supported by NIA R01AG02238.NJ. L.D. was supported by R01AG059874 and R01MH117601. P.M.T. and S.I.T. were supported by NIH R01AG058854 to the ENIGMA World Aging Center, U01AG068057, R01MH116147, P41EB015922, and a Zenith Grant (ZEN-20-644609) from the U.S. Alzheimer's Association. P.R.S. was supported by National Health and Medical Research Council, Australia grants 1037196, 1063960 and 1176716. R.A.-A. is funded by a Miguel Servet contract from the Carlos III Health Institute (CP18/00003), carried out on Fundación Instituto de Investigación Marqués de Valdecilla. P.G.F. received funding from the German Research Foundation, the European Union and the Federeal Ministry of Science. R.A.B. was supported by the European Research Council. S.I.B. was supported by FAPESP 2016/04983-7, FAPESP 2011/50740-5 and INCT (CNPq/FAPESP) 2014/50917-0. S.E.F. was supported by the Max Planck Society. S.E.M. was supported by NHMRC APP1103623, APP1172917 and APP1158127. S.H.W. was supported by DFG FOR2107 Wi3439/3-2 and BMBF Neuron ERANET Synschiz 01EW1810. S.L.H. was supported by the University of Bergen, the Trond Mohn Research Foundation and Helse Vest. S.R.C. was supported by a Sir Henry Dale Fellowship jointly funded by the Wellcome Trust and the Royal Society (grant 221890/Z/20/Z). T.E.l. was funded by the Research Council of Norway, the South-Eastern Norway Regional Health Authority, Oslo University Hospital and a research grant from Mrs. Throne-Holst. T.H. was supported by grants from the Interdisciplinary Center for Clinical Research (IZKF) of the Medical Faculty of Münster (grant MzH 3/020/20) and the German Research Foundation (DFG grants HA7070/2-2, HA7070/3 and HA7070/4). T.J. was supported by the National Natural Science Foundation of China (81801773, 81930095 and 91630314), the Shanghai Pujiang Project (18PJ1400900), the Key Project of Shanghai Science and Technology Innovation Plan (16JC1420402), the Shanghai Municipal Science and Technology Major Project (2018SHZDZX01) and the Zhangjiang lab. T.R.M. was supported by the Medical Research Council (UK). T.W. was supported by the Netherlands Organization for Health Research and Development (ZonMw) TOP project (91211021) and Sophia Children's Hospital Foundation (Stichting Vrienden van het Sophia) project S18-68. V.M. was supported by CONICYT fellowships 21180871. U.F.M. was supported by the Throne-Holst Foundation. V.M.S. was supported by the Research Council of Norway (grant 223273 NORMENT). W.S.K. was supported by NIA grants R01 AG050595, R01 AG022381, R01AG060470 and R01 AG054002 and NIAAA grant R01 AA026881.

Author contributions

Conceptualization: B.F., C.E.F., H.E.H., M.S.P., N.J., P.M.T., R.M.B., S.E.M. and W.S.K. Central analysis and coordination: B.F., C.D.W., E. Sprooten, H.E.H., H.G.S., M.K., K.L.G., N.J., P.M.T., R.M.B., S.E.M. and S.I.T. Core writing team: B.F., H.E.H., K.L.G., M.K., N.J., P.M.T., R.M.B. and S.E.M. Visualization: J. Teeuw, M.K. and R.M.B. Cohort principle investigators: A.H., A.J., A.K., A.L.W.B., A.P.J., B.C.F., B.T.B., B.W.J.H.P., C. Arango, C.M., D. Ames, D.I.B., E.G.J., F.N., G.A.S., G. Schumann, H.B., H.E.H., H.F., H.G., H.H.H.A., H.J.G., H.L., H.W., I.A., I.N., J.-L.M., J.H., J.H.V., J.K. Buitelaar, J.M.F., J.O., J. Trollor, K.A., K.S., L.H.v.d.B., L.P., L.T.W., M.A.I., M.H.J., M.J.W., M.N.S., M.S.K., O.A.A., P.A.G., P.B.M., P.G.F., P.J.H., P.M.P., P.R.S., P.S., P.S.S., R.A.B., R.A.O., R.L.M., R.M.M., R.S.K., R.W., S. Caspers, S. Cichon, S.E.F., S.I.B., S.R.C., T.B., T.E.l., T. Espeseth, T.H., T. Kircher, T.W., U.D., U.F.M. and W.C. Imaging data collection: A.G., A.L.W.B., A.P.J., A.Z., A.v.d.L., B.I., B.M., C.A.M., C.A.H, C.D.-C., C.J., C.M., D. Ames, D.G., D.I.B., D.J.H., D.M.C., D.T.-G., E.A., E. Bøen, E.G.J., E. Shumskaya, F.N., F. Stein, G.J.B., G.R., G. Sudre, H.-J.W., H.F., H.H.H.A., I.A., I.A.B., J.-L.M., J.G., J.H., J.H.F., J. Janssen, J.M.F., J.M.W., J.R., J. Trollop, K.A., K.D., K.S., L.H.v.d.B., L.T.W., M.A.I., M.E.B., M.G.J.C.K., M.J.W., M.L.P.M., M.N.S., M.S.K., N.E.M.v.H., N.O., N.S., O.A.A., P.A.G., P.D., P.M.P., P.R.J., P.S., R.A.-A., R.B., R.K.L., R.R., S. Desrivières, S.H., S.M., T.R.M., T.W., T.W.M., U.D., V.O.G., W.H. and W.W. Genetic data collection: A.J.F., A.L.W.B., B.M., B.T.B., B.W.J.H.P., C. Arango, C.D.-C., C.M., D.I.B., D.W.M., E.A., E.G.J., F.N., F. Stein, F. Streit, G.H., G. Sudre, H.F., H.H.H.A., I.A.B., J.-L.M., J.B.J.K., J.G.-P., J.H., J.J.H., J.M.F., J.R., J. Trollop, J.V.-B., K.A.M., K.S., L.H.v.d.B., M.D.F., M.J.W., M.L.P.M., M.L.S., M.M.N., M.N.S., M.R., M.S.K., N.S., O.A.A., P.D., P.M.P., P.R.S., P.S., R.A.O., R.R., S. Cichon, S. Desrivières, S.E.F., S.H.W., S.I.B., S.L.H., S.M., T.R.M., T.W.M., U.D. and V.M.S. Imaging data analysis: A.G., A.H.Z., A.P.J., A. Thalamuthu, A.Z., B.J.O., B.M., C. Alloza, C.G.D., C.J., C.L.d.M., D. Alnæs, D.G., D.K., D.M.C., D.T.-G., E. Blok, E.E.L.B., E. Shumskaya, E. Sprooten, F.N., G.B., G. Sudre, G.V.R., H.-J.W., H.J.G., I.A., I.A.B., J. Jiang, J.K. Bright, J.M.W., K.S., K.W., L.K.M.H., L.N., L.T.W., M.A., M.A.H., M.G.J.C.K., M.S.K., N.A.C., N.E.M.v.H., N.J., N.S., N.T., R.B., R.C.W.M., R.M.B., R.R., S. Ciufolini, S.I.T., S.J.H., S.M.C.d.Z., S.R.C., S.T., T.J., T. Karali, T.W., U.D., V.M., W.H. and W.W. Genetic data analysis: A.J.F., A. Teumer, A. Thalamuthu, B.M., B.T.B., C.G.D., C.L.d.M., D.v.E., D.v.d.M., E. Blok, E. Sprooten, E.V., F. Streit, G.B., G. Davies, G. Donohoe, G. Sudre, G.V.R., J.B., J.B.J.K., J.G.-P., J.L.S., J.M.F., J.P.O.F.T.G., J. Teeuw, K.R., K.S., L.D., L.M.O.L., M.A.I., M.J.K., M.L.S., M.R., N.J., N.J.A., P.R.J., R.M.B., R.M.T., S. Dalvie, S.E.M., S.H.W., S.I.B., S.L.H., S.M.C.d.Z., S.P., T.J. and Y.M.

Competing interests

B.F. has received speaking fees from MEDICE Arzneimittel Pütter GmbH & Co. B.W.J.H.P. has received research funding from Jansen Research and Boehringer Ingelheim. C.A. has been a consultant to or has received honoraria or grants from Acadia, Angelini, Gedeon Richter, Janssen Cilag, Lundbeck, Minerva, Otsuka, Roche, Sage, Servier, Shire, Schering Plough, Sumitomo Dainippon Pharma, Sunovion and Takeda. C.D.W. is an employee of Biogen, Inc. D.J.S. has received research grants and/or consultancy honoraria from Lundbeck and Sun. G.J.B. receives honoraria for teaching from GE Healthcare. H.B. is on the Advisory Board Nutricia Australia. H.E.H. has received travel fees for membership of the Steering Committee of the Lundbeck Foundation Center for Clinical Intervention and Neuropsychiatric Schizophrenia Research and for two presentations from Philips. These concerned activities were unrelated to the submitted work. H.J.G. has received travel grants and speaker's honoraria from Fresenius Medical Care, Neuraxpharm, Servier and Janssen Cilag as well as research funding from Fresenius Medical Care. L.P. has served as an advisor or consultant to Shire, Takeda and Roche. L.P. has also received speaking fees from Shire and Infectopharm. The present work is unrelated to these relationships. M.H.J. received grant support from the Brain and Behavior Foundation (NARSAD) Independent Investigator grant 20244. M.M.N. has received fees for memberships in Scientific Advisory Boards from the Lundbeck Foundation and Robert Bosch Stiftung and for membership in the Medical-Scientific Editorial Office of the Deutsches Ärzteblatt. M.M.N. was reimbursed travel expenses for a conference participation by Shire Deutschland GmbH. M.M.N. receives salary payments from Life & Brain GmbH and holds shares in Life & Brain GmbH. All these concerned activities are outside the submitted work. N.J. and P.M.T. are multiple principal investigators of a research grant from Biogen, Inc for work unrelated to the contents of this manuscript. O.A.A. has received speaker's honoraria from Lundbeck and has been a consultant for HealthLytix. P.S.S. reports on/off payment for an advisory board meeting of Biogen. T.B. served in an advisory or consultancy role for Lundbeck, Medice, Neurim Pharmaceuticals, Oberberg GmbH, Shire and Infectopharm. T.B. also received conference support or speaker's fees from Lilly, Medice and Shire and received royalties from Hogrefe, Kohlhammer, CIP Medien and Oxford University Press. The present work is unrelated to these relationships. T.E.l. has received speaker's fees from Lundbeck. T.R.M. has received honoraria for speaking and chairing engagements from Lundbeck, Janssen and Astellas. Other authors declare no conflicts of interest.

Additional information

Extended data is available for this paper at https://doi.org/10.1038/s41593-022-01042-4.

Supplementary information The online version contains supplementary material available at https://doi.org/10.1038/s41593-022-01042-4.

Correspondence and requests for materials should be addressed to Rachel M. Brouwer or Hilleke E. Hulshoff Pol.

Peer review information *Nature Neuroscience* thanks Janine Bijsterbosch, Andrew McIntosh and the other, anonymous, reviewer(s) for their contribution to the peer review of this work.

Reprints and permissions information is available at www.nature.com/reprints.

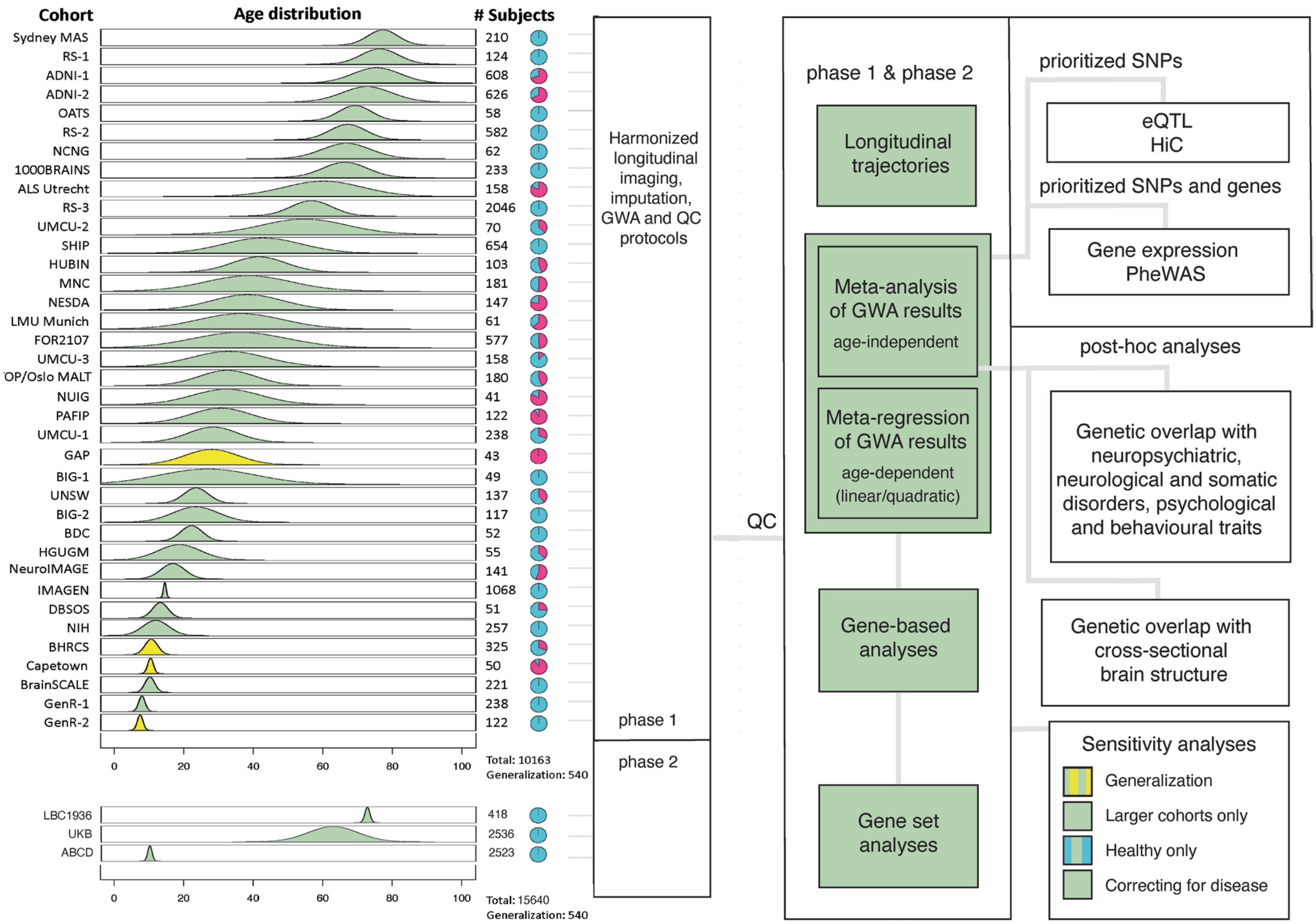

Extended Data Fig. 1 | Demographics and analysis. Overview of demographics (left). Per cohort, an age distribution is displayed, based on mean and standard deviation of the age at baseline. Cohorts of European ancestry are displayed in green, non-European cohorts are displayed in yellow. On the right, the total number of included subjects is displayed and a pie-chart of the distribution of diagnostic groups (pink) and subjects not belonging to diagnostic groups - often healthy subjects (aqua). Overview of analysis pipeline (right).

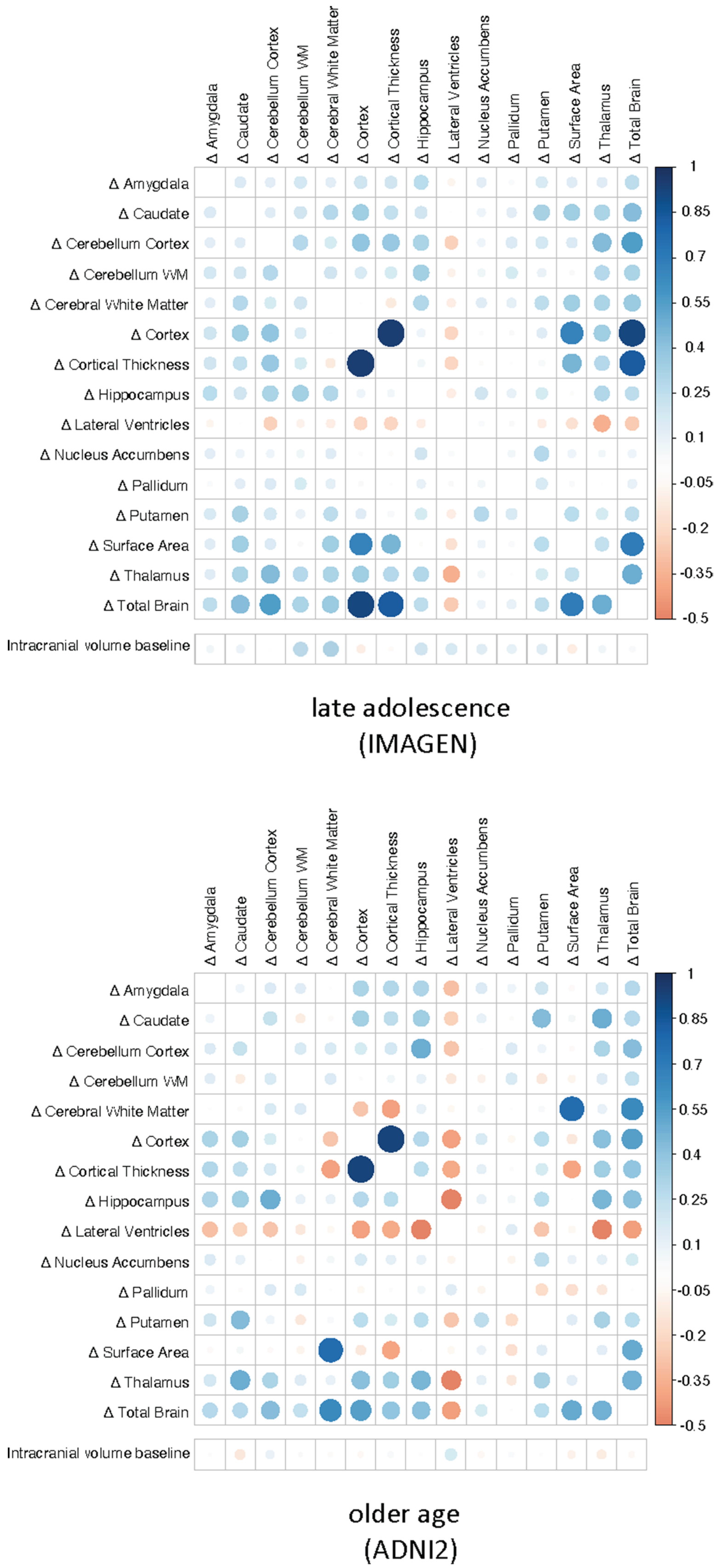

Extended Data Fig. 2 | Correlations between change rates. Pearson correlations between rates of change and between baseline intracranial volume and rates of change in the largest adolescent cohort (top, N = 1068) and the largest cohort in older age (bottom, N = 624) in phase 1. The size of the correlations is displayed by color and size of the circles.

nature portfolio

Corresponding author(s): Rachel M Brouwer
Hilleke E Hulshoff Pol

Last updated by author(s): 15-02-2022

Reporting Summary

Nature Portfolio wishes to improve the reproducibility of the work that we publish. This form provides structure for consistency and transparency in reporting. For further information on Nature Portfolio policies, see our Editorial Policies and the Editorial Policy Checklist.

Statistics

For all statistical analyses, confirm that the following items are present in the figure legend, table legend, main text, or Methods section.

n/a	Confirmed	
☐	☒	The exact sample size (n) for each experimental group/condition, given as a discrete number and unit of measurement
☐	☒	A statement on whether measurements were taken from distinct samples or whether the same sample was measured repeatedly
☐	☒	The statistical test(s) used AND whether they are one- or two-sided *Only common tests should be described solely by name; describe more complex techniques in the Methods section.*
☐	☒	A description of all covariates tested
☐	☒	A description of any assumptions or corrections, such as tests of normality and adjustment for multiple comparisons
☐	☒	A full description of the statistical parameters including central tendency (e.g. means) or other basic estimates (e.g. regression coefficient) AND variation (e.g. standard deviation) or associated estimates of uncertainty (e.g. confidence intervals)
☐	☒	For null hypothesis testing, the test statistic (e.g. F, t, r) with confidence intervals, effect sizes, degrees of freedom and P value noted *Give P values as exact values whenever suitable.*
☒	☐	For Bayesian analysis, information on the choice of priors and Markov chain Monte Carlo settings
☒	☐	For hierarchical and complex designs, identification of the appropriate level for tests and full reporting of outcomes
☐	☒	Estimates of effect sizes (e.g. Cohen's d, Pearson's r), indicating how they were calculated

Our web collection on statistics for biologists contains articles on many of the points above.

Software and code

Policy information about availability of computer code

Data collection	No software was used to collect data.
Data analysis	Cohort level data was analysed using Freesurfer for image processing (Fischl et al., 2002; 2004; Reuter et al., 2012, versions 5.1/5.3/6.0, see Supplementary Table 2 for details). The cohort-level genetic data was analysed using the Michigan imputation server (https://imputationserver.sph.umich.edu/; Das et al., 2016), Sanger imputation server (McCarthy et al., 2016), minimac (Howie et al., 2012; release 2013-07-17) or IMPUTE4 (Bycroft et al., 2018) and raremetalworker (Feng et al., 2014; versions 4.13.6, 4.13.8, 4.13.9, 4.14.1) or rvtests (Zhan et al., 2016; release 2016-06-13) for GWAS, see Supplementary Table 3 for details. The meta-analysis/meta-regression was performed using METAL (Willer et al., 2010, release 2011-03-25), R (http://www.r-project.org/, version 3.6.1). Figures were created using phenogram (http://visualization.ritchielab.org; web-application, accessed on 30-11-2021), FUMA (Watanabe et al., 2017, web-application, accessed Aug 2021) and locuszoom (Pruim et al., 2011, version 1.3). The code for processing of individual cohorts (including imaging and QC, imputation and GWAS protocol) can be found on http://enigma.ini.usc.edu/ongoing/enigma-plasticity-working-group/. Code for the meta-regression is available through Github https://github.com/RMBrouwer/GWAS_meta_regression.

For manuscripts utilizing custom algorithms or software that are central to the research but not yet described in published literature, software must be made available to editors and reviewers. We strongly encourage code deposition in a community repository (e.g. GitHub). See the Nature Portfolio guidelines for submitting code & software for further information.

Data

Policy information about availability of data

All manuscripts must include a data availability statement. This statement should provide the following information, where applicable:

- Accession codes, unique identifiers, or web links for publicly available datasets
- A description of any restrictions on data availability
- For clinical datasets or third party data, please ensure that the statement adheres to our policy

This work is a meta-analysis. Upon publication, the meta-analytic results will be made available from the ENIGMA consortium webpage (http://enigma.ini.usc.edu/research/download-enigma-gwas-results). Cohort level data can be shared upon request, after permission of cohort principle investigators. Individual level data can be shared with interested investigators, subject to local and national ethics regulations and legal requirements that respect the informed consent forms and national laws of the country of origin of the persons scanned. Figures that contain cohort level (meta) data: Figure 1, 2, Extended data Figures 1,2, Supplementary Figures 1,3,8,10.

Public data used in this work include the ABCD cohort (data release 3.0, accessible through https://nda.nih.gov/abcd; http://dx.doi.org/10.15154/1519007), ADNI cohort (accessible through adni.loni.usc.edu), and the UK biobank cohort (data request 11559, https://www.ukbiobank.ac.uk).

Field-specific reporting

Please select the one below that is the best fit for your research. If you are not sure, read the appropriate sections before making your selection.

☒ Life sciences ☐ Behavioural & social sciences ☐ Ecological, evolutionary & environmental sciences

For a reference copy of the document with all sections, see nature.com/documents/nr-reporting-summary-flat.pdf

Life sciences study design

All studies must disclose on these points even when the disclosure is negative.

Sample size	Sample size was determined based on availability of data.
Data exclusions	All data sent in was analyzed. In sensitivity analyses, we excluded cohorts that (after quality control) did not meet the preset inclusion criteria of N > 75 and at least 6 months interval between measurements.
Replication	We sought replication through a rolling meta-analysis approach. For our main findings, 3 out of 6 SNPs and 4 out of 6 genes that were genome-wide significant in phase 1 were also genome-wide significant in phase 2.
Randomization	This was an observational study, randomization does not apply.
Blinding	This was an observational study, blinding does not apply.

Reporting for specific materials, systems and methods

We require information from authors about some types of materials, experimental systems and methods used in many studies. Here, indicate whether each material, system or method listed is relevant to your study. If you are not sure if a list item applies to your research, read the appropriate section before selecting a response.

Materials & experimental systems

n/a	Involved in the study	
☒	☐	Antibodies
☒	☐	Eukaryotic cell lines
☒	☐	Palaeontology and archaeology
☒	☐	Animals and other organisms
☐	☒	Human research participants
☒	☐	Clinical data
☒	☐	Dual use research of concern

Methods

n/a	Involved in the study	
☒	☐	ChIP-seq
☒	☐	Flow cytometry
☐	☒	MRI-based neuroimaging

Human research participants

Policy information about studies involving human research participants

Population characteristics	We included 15,100 subjects aged 4 to 99 (49% female, 14% patients; including schizophrenia, bipolar disorder, MDD, ALS, HIV)

Recruitment	This is a meta-analysis, subjects were recruited by the individual sites. Sites were recruited through the ENIGMA consortium, and by invitations through email after publications on longitudinal MRI data. In addition, we used publicly available data.
Ethics oversight	Ethics approval for meta-analyses within the ENIGMA consortium was granted by the QIMR Berghofer Medical Research Institute Human Research Ethics Committee in Australia (approval: P2204).

Note that full information on the approval of the study protocol must also be provided in the manuscript.

Magnetic resonance imaging

Experimental design

Design type	Not applicable, structural imaging
Design specifications	Not applicable, structural imaging
Behavioral performance measures	Not applicable, structural imaging

Acquisition

Imaging type(s)	structure
Field strength	1.5T and 3T
Sequence & imaging parameters	Varying between cohorts. Details on acquisition per cohort are given in supplementary table 2.
Area of acquisition	Whole brain

Diffusion MRI ☐ Used ☒ Not used

Preprocessing

Preprocessing software	Freesurfer 5.3 or Freesurfer 6.0 (Fischl et al., 2002; 2004).
Normalization	Not normalized: we are investigating longitudinal change and each subject serves as his/her own control.
Normalization template	Not normalized.
Noise and artifact removal	Not applicable, structural imaging
Volume censoring	Not applicable, structural imaging

Statistical modeling & inference

Model type and settings	Mass univariate, genome-wide associations taking family relatedness into account (raremetalworker; Feng et al., 2014).
Effect(s) tested	Not applicable

Specify type of analysis: ☐ Whole brain ☒ ROI-based ☐ Both

Anatomical location(s)	Automatic labeling of the Freesurfer suite was used.
Statistic type for inference (See Eklund et al. 2016)	Not applicable
Correction	Bonferroni correction based on the number of independent input variables (Nyholt 2004).

Models & analysis

n/a	Involved in the study
☒	☐ Functional and/or effective connectivity
☒	☐ Graph analysis
☒	☐ Multivariate modeling or predictive analysis